BNWL-B-281

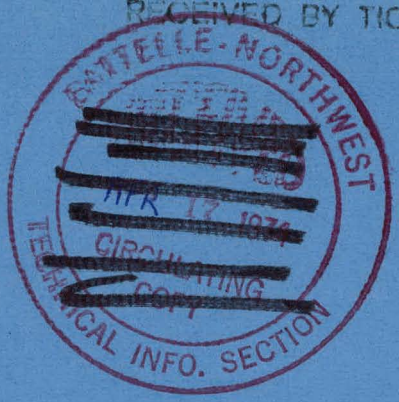

FINAL REPORT ON ARPA FISSION YIELD PROJECT WORK AT BATTELLE-NORTHWEST APRIL 1970 - APRIL 1973

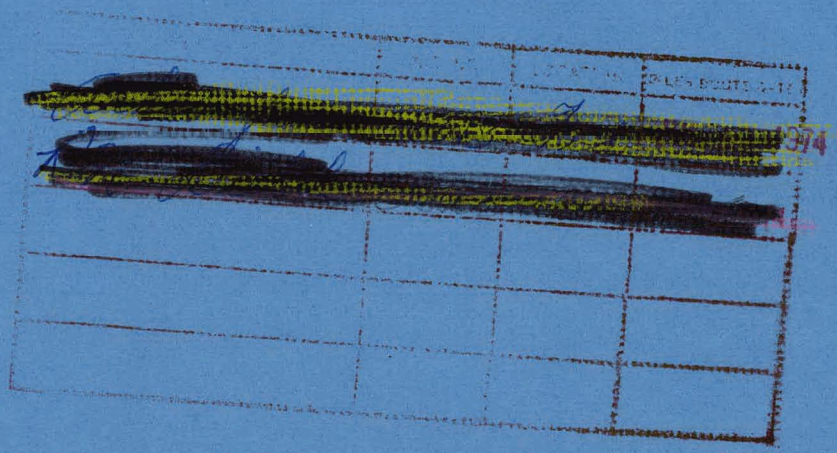

BNWL-B-281

DISCLAIMER

FINAL REPORT ON ARPA FISSION YIELD PROJECT WORK AT BATTELLE-NORTHWEST APRIL 1970 - APRIL 1973(a)

N. E. Ballou, J. H. Kaye, P. L. Reeder
J. J. Stoffels, R. A. Anderl

Battelle
Pacific Northwest Laboratories
Richland, Washington 99352

(a) This paper is based on work performed under United States Atomic Energy Commission Contract AT(45-1)-1830 and under the sponsorship of the Advanced Research Projects Agency of the Department of Defense, ARPA Order No. 1590.

TABLE OF CONTENTS

FINAL REPORT ON ARPA FISSION YIELD PROJECT WORK, APRIL 1970 - APRIL 1973

I. INTRODUCTION

The overall objective of this project has been to measure the independent and cumulative fission yields of selected halogen and rare gas nuclides for application to characterization of underground nuclear detonations. The studies have included fission yield measurements for thermal, fission spectrum, and 15 MeV neutron-induced fission events. Target materials included ^{235}U, ^{238}U and ^{239}Pu.

The research effort was divided into two basic parts. In one part, the nuclides of interest were separated radiochemically and determined by gamma-ray spectrometry. This approach provides information on the independent and cumulative yields of nuclides with half-lives of a few seconds or greater. The second part of our effort involved the use of on-line mass separation techniques. This approach yields information on independent fission yields of nuclides with half-lives ranging down to fractions of a second and provides data on all significant isotopes of a given fission product element in one set of measurements.

At the sponsor's request, the main effort in the radiochemistry program was centered on measurements of the cumulative fission yield of ^{89}Kr, and work on independent yield measurements of bromine isotopes which had been initiated

originally was suspended at the end of the first project-year. Cumulative fission yields of ^{89}Kr were measured for thermal-neutron fission of ^{239}Pu and for fission-spectrum and 15-MeV neutron fission of ^{235}U, ^{238}U and ^{239}Pu. In addition, cumulative fission yields of the other rare gas radionuclides, ^{85m}Kr, ^{87}Kr, ^{88}Kr, ^{137}Xe, ^{138}Xe, were measured for the same fission type events. Fractional independent yields of ^{89}Rb and ^{138}Cs were also measured for a limited number of fission systems.

On-line mass spectrometer facilities were established at a Van de Graaff accelerator and at a nuclear reactor. Measurements were made of relative independent fission yields of rubidium isotopes of masses 89 through 97 and of cesium isotopes of masses 139 through 145. Techniques for generation and measurement of negative ions of bromine and iodine fission product isotopes were developed and demonstrated.

II. RADIOCHEMISTRY

1. Introduction

This is the final technical progress report on the ARPA fission yield project work, and thus the overall radiochemical study will be reviewed briefly. The radiochemical studies for this project were begun 20 April, 1970. Initially a rapid sample transfer system for neutron irradiations was installed at the Hanford KE production reactor, 30 miles northwest of the Battelle-Northwest Laboratories. Radiochemical studies were carried out to develop procedures for rapid separation of bromine from other fission products and from the bromine precursors arsenic and selenium. A satisfactory procedure was developed based on decomposition of uranyl bromate which resulted

in reasonable bromine recovery in as little as two seconds. However, further work on bromine chemistry was terminated due to a request from ARPA that studies of rare gas fission yields be given higher priority, with emphasis to be given to determination of the cumulative fission yields of ^{89}Kr for fission of ^{235}U and ^{239}Pu with thermal neutrons and of ^{235}U, ^{238}U and ^{239}Pu with fission-spectrum and 15-MeV neutrons.

In January, 1971 the KE production reactor was permanently shut down, so facilities for rapid thermal neutron irradiations were installed at the TRIGA reactor of Washington State University (WSU) at Pullman, Washington, 150 miles from Richland. The technique used for rare gas yield studies at WSU consisted of irradiation of 30-50 mg of natural uranium stearate in sealed quartz ampoules for approximately 30 seconds in a flux of 2.5×10^{12} $n \cdot cm^{-2} \cdot sec^{-1}$. After irradiation the ampoule was crushed and the fission gases were swept into a counting cell. The amount of each rare-gas isotope was determined by Ge(Li)-diode gamma-ray spectrometry. Computer programs were developed to process the large amount of experimental data. A modified version of the GASPAN program was used to determine photopeak energies and areas.

The cumulative fission yield of ^{89}Kr was first determined for the case of thermal-neutron irradiation of ^{235}U. Then methods were developed which also allowed estimation of the cumulative yields of ^{85m}Kr, ^{87}Kr, ^{88}Kr, ^{137}Xe and ^{138}Xe. Experiments to determine the fractional independent yields of ^{89}Rb and ^{138}Cs were also done. In October 1972 irradiations of ^{239}Pu with thermal neutrons were made at WSU, and rare-gas

cumulative fission yields of the above-mentioned radionuclides were measured. The experimental apparatus was then modified extensively in order to permit irradiation of gram-sized quantities of both uranyl and plutonyl stearate with fission-spectrum and 15-MeV neutrons. The equipment was moved to the Lawrence Livermore Laboratory in December, 1972. Plutonyl stearate was next synthesized for the rare-gas yield studies. Between December, 1972 and April, 1973 irradiations of the target materials ^{235}U, ^{238}U and ^{239}Pu were made with fission-specturm neutrons at the Lawrence Livermore Laboratory (LLL) Fast Neutron Irradiation Facility (FNIF) and with 15-MeV neutrons at the LLL Isolated Core Transformer (ICT) facility. Additional studies included determination of independent and cumulative yields of ^{138}Xe and ^{138}Cs for the cases of irradiation of ^{239}Pu with fission-spectrum and 15-MeV neutrons and of ^{235}U with 15-MeV neutrons.

After completion of the irradiations at Livermore, the equipment was returned to Richland. Several capsules and a vial containing plutonyl stearate were donated to the Los Alamos Radiochemistry group to be used by Kurt Wolfsberg in his rare-gas fission yield studies.

The data presented in this report is in final form and summarizes the results of the ARPA radiochemical studies. All of the objectives of the rare gas part of the fission yield study as outlined in the proposal for April 1972-April 1973 have been accomplished. In addition, yields of several other important radionuclides were simultaneously determined. Work

on the lowest priority item in the proposal, studies of ^{85}Br fission yields, was not initiated.

In the following sections, we present results obtained since the last quarterly report and a summary of all fission yield results obtained by this research project.

2. Progress on Radiochemical Studies Since Last Quarterly Report

The last quarterly technical progress report[1] covered the period 1 November 1972 through 31 January 1973. Since that time plutonium irradiations at LLL were conducted for measurement of rare-gas yields and the independent and cumulative yields of ^{138}Xe and ^{138}Cs. Additional measurements of rare-gas yields were made for the case of thermal neutron irradiation of ^{235}U. All data processing has been completed and equipment returned to Richland.

In the following sub-sections, we describe the fission yield measurements made since the last quarterly report.

A. Cumulative Fission Yields of ^{85m}Kr, ^{87}Kr, ^{88}Kr, ^{89}Kr, ^{137}Xe and ^{138}Xe for Fission of ^{239}Pu with Fission-Spectrum Neutrons

Details regarding the preparation of plutonyl stearate and fabrication of sintered-frit capsules for irradiation of stearate powder were given in the previous report[1]. Special precautions were taken for irradiation of ^{239}Pu, since relatively large quantities of ^{239}Pu (0.5g ^{239}Pu per capsule) as very fine powder were being handled. An alpha probe (PAM) was installed inside the glove box, and a feed-through connector was used so that readout and power supply for the instrument were outside the glove box. A sintered-frit filter was employed down-stream from the irradiation capsule puncturing

device so that plutonium would not be swept into the counting cell in the event that powder escaped from a capsule. A wooden-framework "tent" of polyethylene 7 ft high by 4 ft wide by 5 ft deep was fastened to the hood in which the glove box was placed to act as an added barrier in case plutonium escaped from the glove box. After each irradiation the counting cell, puncturing device, and inner and outer irradiation capsules were monitored for alpha activity and a swipe sample of the inner capsule was taken. Prior to irradiation each capsule assembly was checked for air leakage by means of underwater immersion in a vacuum desiccator. Leaky O-ring seals could be readily detected in this manner since a stream of air bubbles would evolve when the desiccator was evacuated. None of the plutonium-containing capsule assemblies leaked. The sintered-frit type capsules proved to be highly safe and reliable for irradiation of plutonyl stearate.

A total of nine ^{239}Pu irradiations were made in the Fast Neutron Irradiation Facility for rare-gas fission yield studies. For three of these runs, the rare-gas separation was deliberately delayed for 15 minutes after irradiation to allow decay of the rare gas precursors, ^{85}Br and ^{87}Br. It was found that an irradiation interval of one minute resulted in about the same rare-gas activity as a 30-second irradiation of the same quantity of ^{235}U. The capsule assembly was manually transferred from the FNIF "mouse" capsule receiver station through an air lock to the glove box in a radiochemistry laboratory. After the gas sample was collected, it was counted for up to 12 hours with the Ge(Li)-diode spectrometer system.

The results of these irradiations are summarized in Table 13. The values agree rather well with those predicted by Meek and Rider[2], as shown. The greatest discrepancy occurs for ^{138}Xe, and this is discussed in section 2C. General comments on Tables 8-14 are given in section 3.

B. Cumulative Fission Yields of ^{85m}Kr, ^{87}Kr, ^{88}Kr, ^{89}Kr, ^{137}Xe and ^{138}Xe in Fission of ^{239}Pu with 15-MeV Neutrons

The separation procedure for the 15-MeV irradiations of ^{239}Pu was similar to that used for the fission-spectrum neutron irradiations. The most significant difference was that for the 15-MeV runs the BNW pneumatic sample transfer system was used to transfer the sample capsule directly into the glove box, so that the sample did not have to be manually transported. A total of ten ^{239}Pu irradiations were made at the ICT facility for rare-gas fission yield studies. In four of the runs the rare-gas separation was deliberately delayed for 15 minutes after irradiation. Irradiation intervals were two minutes, which yielded about the same rare gas activity as one-minute irradiations at the FNIF.

Results of the 15-MeV irradiations of ^{239}Pu are summarized in Table 14. Values of the cumulative fission yield of the reference nuclides ^{88}Kr and ^{138}Xe could not be found in the literature. The value for the case of ^{88}Kr was estimated by multiplication of the 88 chain yield value for 14.8 MeV neutron irradiation of ^{239}Pu, 1.63 percent, taken from the recent tabulation of Nethaway[93], by a computed fractional cumulative yield estimate for ^{88}Kr, 0.894, obtained from Wolfsberg[4].

The cumulative yield of ^{138}Xe was determined from the experiments discussed in the next section.

The values obtained for ^{85m}Kr and ^{87}Kr are low relative to the comparison values by 15 and 17 percent respectively. The comparison values are based on Wolfsberg's[4] calculated fractional yields and Nethaway's[3] chain yields and may involve uncertainty of this magnitude. The results for ^{88}Kr and ^{89}Kr are close to the comparison values. Those for ^{137}Xe and ^{138}Xe are very low in relation to the comparison values, and this is discussed in the following pages.

C. Determination of the Fractional Independent and Cumulative Yields of 138-Chain Members for Fission Spectrum and 15 MeV Neutron Irradiation of ^{239}Pu

An examination of the published literature reveals that there is very little data available for estimation of the cumulative yields of ^{88}Kr or ^{138}Xe for either fission spectrum or 15 MeV neutron irradiation of ^{239}Pu. For the case of fission-spectrum neutron-induced fission, estimates are given in Meek and Rider's fission yield tabulation[2] for the 88-mass chain, but no experimental values are referenced except for ^{88}Sr. For the 138 chain, experimental cumulative yield values for ^{138}Xe, ^{138}Cs and ^{138}Ba are cited[17], but the uncertainties for the ^{138}Xe and ^{138}Cs values are given as 37 and 41 percent respectively. No values are given in Meek and Rider's tabulation for 15 MeV fission of ^{239}Pu. Chain yields for 15 MeV fission of ^{239}Pu have been given by Nethaway[3].

No experimental fractional yield values for ^{88}Kr or ^{138}Xe are published.

We have performed experiments to measure the fractional independent yield of ^{138}Cs, from which the fractional cumulative yield of ^{138}Xe may be computed. Irradiations were performed with both fission-spectrum and 15-MeV neutrons. Plutonyl stearate was irradiated in the capsules described in earlier reports[1,5]. After irradiation the capsule was transferred to a glove box and the outer container was punctured and rare gases were swept out as was done for the rare gas studies. However in this experiment the inner capsule containing the irradiated stearate was gamma counted instead of the emanated fission gases. The ^{138}Cs activity in the sample was thereby determined. A comparison was made of the ^{138}Cs activity for runs in which the gases were flushed out as quickly as possible after irradiation and runs in which puncture of the outer capsule was delayed for up to 80 minutes. In the latter case the ^{138}Cs activity was due to both ^{138}Cs produced directly and ^{138}Cs produced through decay of ^{138}Xe. In the former, most of the ^{138}Cs was due to independent production from ^{239}Pu fission. Two runs of each type were made at the FNIF and two of each were made at the ICT facility. The ^{97}Zr gamma activity in each sample was also measured in order to determine the relative neutron exposure of each capsule. The 1436 keV photopeak of ^{138}Cs was used for the ^{138}Cs activity estimations, and both the 743 and 658 keV photopeaks of ^{97}Zr-^{97}Nb were used for ^{97}Zr estimation.

In order to estimate the ^{138}Xe and ^{138}Cs fractional yields from this experimental data it is necessary to make an assumption

as to the charge distribution for the 138-mass chain. This distribution was assumed to be Gaussian with a width parameter σ of 0.56, as has been estimated for other fission systems by Wahl et al.[6], and as is assumed in the fission yield tabulations of both Meek and Rider[2] and Wolfsberg[4]. A program was written for the UNIVAC 1108 computer in BASIC language to compute fractional independent and fractional cumulative fission yield estimates for ^{138}I, ^{138}Xe and ^{138}Cs based on the above charge distribution assumption and the experimental data. The results are presented in Tables 1 and 2. For the case of fission-spectrum neutron irradiation of ^{239}Pu the calculated values agree very well with Wolfsberg's predictions[4], somewhat better than with Meek and Rider's estimates[2]. For the 15-MeV neutron irradiations the experimental results indicate that the independent fission yield of ^{138}Cs may be higher than Wolfsberg predicts, and that of ^{138}Xe may be lower. This would imply that Z_p, the maximum value of the charge distribution curve for the 138-mass chain, may be higher by 0.78 Z units than Wolfsberg's predicted value of 53.79.

As a check on the experimental method, one pair of irradiations of ^{235}U with 15-MeV neutrons was also made. Comparisons with the tabulations of Meek and Rider and of Wolfsberg are given in Table 3. The ^{138}Cs independent yield value for this case is 14 percent higher than Wolfsberg's value, but the independent yield value for ^{138}Xe, 0.590, agrees well with Wolfsberg's value of .609.

Table 4 shows the effect that a variation in the charge distribution width parameter, σ, would have on the ^{138}I, ^{138}Xe and ^{138}Cs yields for the case of 15 MeV fission of ^{239}Pu. As the charge distribution curve is widened (larger σ), the fractional

TABLE 1. Fractional fission yields for 138-mass chain, ^{239}Pu irradiated with fission-spectrum energy neutrons

	Fractional Independent Yield			Fractional Cumulative Yield		
	this work	Meek & Rider[2]	Wolfsberg[4]	this work	Meek & Rider[2]	Wolfsberg[4]
^{138}I	0.156	0.253	0.148	0.159	0.263	0.150
^{138}Xe	0.625	0.491	0.623	0.784	0.754	0.773
^{138}Cs	0.211	0.245	0.221	0.995	0.999	0.994

TABLE 2. Fractional Fission Yields for 138-Mass Chain ^{239}Pu Irradiated with 15-MeV Neutrons

	Fractional Independent Yield		Fractional Cumulative Yield	
	this work	Wolfsberg[4]	this work	Wolfsberg[4]
^{138}I	0.027	0.066	0.027	0.067
^{138}Xe	0.415	0.546	0.442	0.612
^{138}Cs	0.507	0.368	0.949	0.981

TABLE 3. Fractional fission yields for 138-mass chain, ^{235}U irradiated with 15-MeV neutrons

	Fractional Independent Yield			Fractional Cumulative Yield		
	this work	Meek & Rider[2]	Wolfsberg[4]	this work	Meek & Rider[2]	Wolfsberg[4]
^{138}I	0.097	0.115	0.118	0.098	0.116	0.119
^{138}Xe	0.590	0.627	0.609	0.688	0.743	0.728
^{138}Cs	0.301	0.249	0.264	0.989	0.992	0.992

TABLE 4. Effect of Charge-Distribution Width-Parameter σ on Computed Fission Yield Values for 138-Chain, ^{239}Pu Irradiated with 15-MeV Neutrons

	Independent Fission Yield			Cumulative Fission Yield		
σ	^{138}I	^{138}Xe	^{138}Cs	^{138}I	^{138}Xe	^{138}Cs
0.30	3.10×10^{-4}	.464	.535	3.10×10^{-4}	.464	.999
0.56	.027	.415	.507	.027	.442	.949
0.80	.059	.324	.446	.062	.386	.832
1.0	.068	.255	.382	.075	.330	.712

independent and cumulative yields of Xe and Cs both decrease, whereas if σ is decreased to 0.3 the values increase somewhat.

Although fractional yield values could be determined directly from the ^{138}Cs and ^{97}Zr measurements, the absolute cumulative yield values could not be calculated because the Ge(Li) diode was not calibrated for the conditions under which the capsule was counted. In order to do this calibration, three irradiations were performed in which capsules containing ^{235}U were irradiated for one minute in a thermal neutron flux of about 3×10^{8} $n\text{-}cm^{-2}\text{-}sec^{-1}$. After 80 minutes delay the fission gases were swept out, and ^{138}Cs and ^{97}Zr activities were determined with the Ge(Li) diode under identical conditions to those established for the case of ^{239}Pu targets. For these ^{235}U experiments the cumulative fission yields of both ^{138}Cs and ^{97}Zr are well known. It is thus possible to relate the observed $^{138}Cs/^{97}Zr$ count-rate ratio (extrapolated to time of fission gas separation) to $^{138}Cs/^{97}Zr$ cumulative yield ratio. The factor relating these two ratios can be used with the observed $^{138}Cs/^{97}Zr$ activity ratios for the ^{239}Pu runs to determine the absolute cumulative yield of ^{138}Cs if the ^{97}Zr cumulative yield is known for the case of the ^{239}Pu irradiations. The value 4.82 percent for the ^{97}Zr cumulative yield for fission-spectrum neutron-induced fission of ^{239}Pu was obtained from Nethaway[7]. The value 4.31 percent was used for the case of 15-MeV irradiations, and was also obtained from Nethaway. For the case of thermal neutron irradiations of ^{235}U, cumulative yield values of 5.93 and 6.74 percent were used for ^{97}Zr and ^{138}Cs respectively, (from Meek and Rider).

The absolute fission yield values shown in Table 5 were obtained by use of the experimental $^{138}Cs/^{97}Zr$ data and the fractional yield

TABLE 5. ^{239}Pu Fission Yields for 138-Mass Chain

Neutron Energy	Cumulative Fission Yield (%) this work ^{138}I	^{138}Xe	^{138}Cs	138-chain	literature ^{138}I	^{138}Xe	^{138}Cs	138-chain
fission spectrum	0.92	4.56	5.78	5.81	1.29	3.71[2]	4.92[2]	4.92[2]
15 MeV	0.09	1.51	3.24	3.41	--	--	4.4[7]	4.6[3]

values determined as discussed earlier. The 138-chain yield estimate for the case of fission-spectrum neutron induced fission is 18 percent higher than the value recommended by Meek and Rider. This difference is more than would be expected on the basis of uncertainties in the experimental data, and bears further investigation. The ^{138}Xe absolute cumulative yield value determined from these experiments was used as the ^{138}Xe reference value for computation of rare gas yields presented in Table 13. This table shows that about the same rare gas cumulative yield values were obtained with ^{138}Xe as reference nuclide as with ^{88}Kr (^{88}Kr cumulative yield value 1.37, taken from Meek and Rider)[2]. It thus appears that data from the fission-gas experiments supports the ^{138}Xe cumulative yield value of 4.56.

The ^{138}Cs yield value and 138-chain yield given in Table 5 for the 15 MeV neutron irradiations are very low compared with Nethaway's values[3]. One might thus expect the cumulative yield value for ^{138}Xe, 1.51, to also be low. Examination of Table 14, however, shows that the results calculated with the value 1.51 for the reference nuclide ^{138}Xe are on the average only 7 percent lower than those calculated with ^{88}Kr as reference nuclide. In the latter case the ^{88}Kr value was obtained by multiplication of the 88-chain yield value of Nethaway[3] by the calculated fractional ^{88}Kr yield value of Wolfsberg[4]. Had Nethaway's 138-mass chain yield and Wolfsberg's fractional cumulative ^{138}Xe yield been used to estimate the cumulative yield of the reference nuclide ^{138}Xe, the rare gas yield estimates would have been 74 percent higher than for ^{88}Kr as reference nuclide. Note from Table 14 that the ^{137}Xe cumulative yield estimate is also very low relative to the

comparison value which might be expected if the ^{138}Xe yield is low. Further study of fission yields for the 137 and 138 mass chains for fission-spectrum and 15-MeV neutron-induced fission of ^{239}Pu is needed.

D. Reevaluation of Calibration Factors for Krypton and Xenon Studies

As discussed in an earlier report,[8] because of uncertainties associated with knowledge of photopeak branching fractions, Ge(Li)-diode absolute counting efficiencies, etc., empirical counting rate ratios were established for each given pair of rare-gas photopeaks by means of experiments in which the rare gases were produced and isolated from thermal neutron-irradiated ^{235}U. The factors relating counting rate ratios to relative numbers of atoms were derived from the known fission yield values as given by Meak and Rider. These are shown in Table 7. As a check on these values for the cases of ^{89}Kr and ^{138}Xe the fractional cumulative yields of ^{89}Rb and ^{138}Cs were measured by radiochemical means, and the cumulative yields of ^{89}Kr and ^{138}Xe were calculated from known chain yields to be 4.50 and 6.35 percent respectively[8].

Since considerable changes were made to the original experimental procedure for the irradiations at Livermore, it was decided to re-determine the calibration factors under the experimental conditions at Livermore. Eight irradiations of ^{235}U as uranyl stearate (about 1.5g stearate) were made at the Livermore Pool Type Reactor (LPTR) with thermal neutrons at a well moderated beam port (thermal flux about 3×10^8 $n \cdot cm^{-2} \cdot sec^{-1}$). Targets placed inside the BNW "mouse" capsule were inserted into the beam port by means of a polyethylene rod for one minute exposure. For three of the runs, rare gas separation was delayed for 15 minutes after irradia-

TABLE 6. Cumulative fission yield values for reference nuclides

Target	Neutron Energy	Reference Nuclide	Rare Gas Cumulative Fission Yield (%)	Reference
^{235}U	thermal	^{88}Kr	3.642	[1]
		^{138}Xe	6.235	[1]
	fission-spectrum	^{88}Kr	3.485	[1]
		^{138}Xe	6.228	[1]
	15 MeV	^{88}Kr	3.470	[1]
		^{138}Xe	3.961	[1]
^{238}U	fission-spectrum	^{88}Kr	2.36	[2]
		^{138}Xe	5.908	[1]
	15 MeV	^{88}Kr	2.234	[1]
		^{138}Xe	4.222	[1]
^{239}Pu	thermal	^{88}Kr	1.340	[1]
		^{138}Xe	5.144	[1]
	fission-spectrum	^{88}Kr	1.368	[1]
		^{138}Xe	4.558	[4]
	15 MeV	^{88}Kr	1.457	[3]
		^{138}Xe	1.507	[4]

[1] Meek and Rider[2], recommended c.f.y.

[2] Assumed equal to 88-chain yield value of Flynn and Glendenin[18]

[3] 88-chain yield of Nethaway[3], multiplied by fractional c.f.y. of Wolfsberg[4]

[4] this report, Table 5

Table 7. Values of cumulative fission yields from Meek and Rider[2] for thermal neutron-induced fission of ^{235}U

Nuclide	Cumulative Fission Yield (%)
^{85m}Kr	1.332
^{87}Kr	2.367
^{88}Kr	3.642
^{89}Kr	4.645
^{137}Xe	5.939
^{138}Xe	6.235

tion. Two sets of calibration factors were established, one set to be used with runs in which the rare gases were separated as soon as possible after irradiation, and one set for runs in which separation was delayed. The delayed separation runs were primarily for measurement of ^{85m}Kr and ^{87}Kr which have relatively long-lived precursors.

The new calibration factors are little changed from the previous values. This verifies that major changes to the experiments, such as increasing the amount of uranyl stearate 50 fold over the amount used for the WSU experiments, did not significantly change the results.

The calibration factors previously determined at WSU have been used for the ^{239}Pu irradiations with thermal neutrons since these runs were also carried out at WSU, whereas the new factors have been used for the Livermore irradiations.

3. Summary of Cumulative Fission Yield Estimates from Measurement of Fission Gas Activities

Tables 8-14 summarize the cumulative yield values obtained in these studies for each of the fissioning systems. In each table, cumulative yield estimates for two reference nuclides, ^{88}Kr and ^{138}Xe, were used to obtain the cumulative fission yield values for the other nuclides and for each other. These reference nuclide values are obtained from other experiments or from estimates of other workers. They are summarized in Table 6.

For ^{88}Kr, ^{89}Kr and ^{138}Xe, estimates can be obtained through either measurement of the parent or daughter activities, and estimates are included for both cases. For ^{88}Kr and ^{138}Xe, the cumulative yield estimate is only meaningful if ^{88}Kr is used as reference

TABLE 8. Cumulative fission yields of rare gas nuclides from fission-spectrum neutron-induced fission of Uranium-235

Nuclide Calculated	Nuclide Measured	Cumulative Fission Yield (%) Reference Nuclides ^{88}Kr	^{88}Rb	^{138}Xe	^{138}Cs	Recommended Mean	Literature Values
^{85m}Kr	^{85m}Kr	1.33 ±.01	1.33 ±.01	1.46 ±.04	1.42 ±.04	1.39	1.43 (2)
^{87}Kr	^{87}Kr	2.23 ±.02	2.28 ±.02	2.49 ±.05	2.42 ±.07	2.37	2.56 (2)
^{88}Kr	^{88}Kr	3.49*	3.51	3.63 ±.15	3.62 ±.08	3.55	3.48 (2)
	^{38}Rb	3.45 ±.04	3.49*	3.60 ±.14	3.60 ±.06		
^{89}Kr	^{89}Kr	4.32 ±.12	4.35 ±.12	4.50 ±.17	4.49 ±.11	4.46	4.57 (2) 4.36±.10 (9)
	^{89}Rb	4.40 ±.10	4.43 ±.09	4.58 ±.16	4.57 ±.07		
^{137}Xe	^{137}Xe	5.69 ±.08	5.73 ±.07	5.93 ±.22	5.92 ±.10	5.82	6.14 (2)
^{138}Xe	^{138}Xe	5.98 ±.27	6.02 ±.25	6.23*	6.21 ±.20	6.12	6.23 (2)
	^{138}Cs	5.99 ±.14	6.03 ±.12	6.24 ±.20	6.23*		

*reference values, rounded off from values in Table 6.

TABLE 9. Cumulative fission yields of rare gas nuclides from 15 MeV neutron-induced fission of Uranium-235

Nuclide Calculated	Nuclide Measured	Cumulative Fission Yield (%) Reference Nuclides ^{88}Kr	^{88}Rb	^{138}Xe	^{138}Cs	Recommended Mean	Literature Values
^{85m}Kr	^{85m}Kr	1.70 ±.02	1.67 ±.02	2.05 ±.13	1.94 ±.10	1.84	2.00 (2)
^{87}Kr	^{87}Kr	2.48 ±.05	2.43 ±.02	2.86 ±.04	2.89 ±.05	2.67	2.95 (2) 2.82±.08 (10)
^{88}Kr	^{88}Kr	3.47*	3.40 ±.04	4.00 ±.11	4.03 ±.15	3.76	3.47 (2) 2.85±0.11 (10)
	^{88}Rb	3.54 ±.04	3.47*	4.08 ±.06	4.12 ±.05		
^{89}Kr	^{89}Kr	3.72 ±.12	3.64 ±.14	4.29 ±.19	4.32 ±.19	4.04	3.62 (2) 4.07±.16 (10)
	^{89}Rb	3.82 ±.11	3.74 ±.04	4.40 ±.07	4.40 ±.07		
^{137}Xe	^{137}Xe	4.15 ±.09	4.06 ±.04	4.78 ±.07	4.82 ±.09	4.45	4.91 (2) 4.78±.20 (10)
^{138}Xe	^{138}Xe	3.44 ±.12	3.36 ±.07	3.96*	3.99 ±.08	3.67	3.96 (2) 4.07±1.31 (11)+
	^{138}Cs	3.41 ±.17	3.33 ±.05	3.93 ±.08	3.96*		4.48±.26 (10)

+experimental value updated by Meek and Rider

*reference values, rounded off from values in Table 6.

TABLE 10. Cumulative fission yields of rare gas nuclides from fission-spectrum neutron-induced fission of Uranium-238

Nuclide Calculated	Nuclide Measured	Cumulative Fission Yield (%) Reference Nuclides ^{88}Kr	^{88}Rb	^{138}Xe	^{138}Cs	Recommended Mean	Literature Values
^{85m}Kr	^{85m}Kr	0.78 ±.01	0.77 ±.01	0.76 ±.02	0.75 ±.02	0.76	0.81 (2)
^{87}Kr	^{87}kr	1.56 ±.02	1.56 ±.03	1.54 ±.03	1.51 ±.04	1.54	1.42 (2)
^{88}Kr	^{88}Kr	2.36*	2.36 ±.04	2.32 ±.06	2.28 ±.06	2.33	2.36 (18) 1.68 (2)
	^{88}Rb	2.36 ±.04	2.36*	2.32 ±.06	2.28 ±.06		1.72±.34 (12)
^{89}Kr	^{89}Kr	2.97 ±.14	3.02 ±.15	2.79 ±.16	2.87 ±.17	2.95	3.01 (2) 2.63 (9)
	^{89}Rb	3.04 ±.15	3.09 ±.15	2.85 ±.17	2.93 ±.14		
^{137}Xe	^{137}Xe	6.36 ±.16	6.46 ±.17	5.96 ±.24	6.14 ±.25	6.05	5.95 (2)
^{138}Xe	^{138}Xe	6.02 ±.14	6.01 ±.15	5.91*	5.81 ±.14	5.99	5.91 (2)
	^{138}Cs	6.11 ±.15	6.10 ±.15	6.00 ±.14	5.91*		

*reference values, rounded off from values in Table 6.

TABLE 11. Cumulative fission yields of rare gas nuclides from 15 MeV neutron-induced fission of Uranium-238

Nuclide Calculated	Nuclide Measured	Cumulative Fission Yield (%) Reference Nuclides ^{88}Kr	^{88}Rb	^{138}Xe	^{138}Cs	Recommended Mean	Literature Values
^{85m}Kr	^{85m}Kr	0.96 ±.01	0.96 ±.02	1.00 ±.04	0.96 ±.05	0.97	0.98 (2) 1.05±.04 (13)
^{87}Kr	^{87}Kr	1.57 ±.02	1.57 ±.04	1.64 ±.06	1.56 ±.07	1.59	1.85 (2) 1.69±.05 (10)
^{88}Kr	^{88}Kr	2.23*	2.22 ±.04	2.11 ±.04	2.23 ±.05	2.20	2.23 (2) 1.84±.06 (10)
	^{88}Rb	2.25 ±.04	2.23*	2.12 ±.02	2.24 ±.05		
^{89}Kr	^{89}Kr	2.82 ±.12	2.81 ±.11	2.67 ±.10	2.82 ±.13	2.77	2.83 (2) 2.57±.08 (10)
	^{89}Rb	2.80 ±.06	2.79 ±.04	2.65 ±.03	2.80 ±.06		
^{137}Xe	^{137}Xe	4.70 ±.17	4.68 ±.13	4.44 ±.11	4.70 ±.22	4.63	5.44 (2) 5.04±.11 (10)
^{138}Xe	^{138}Xe	4.47 ±.08	4.45 ±.03	4.22*	4.46 ±.09	4.28	4.22 (2) 4.16±.69 (11)+
	^{138}Cs	4.23 ±.10	4.20 ±.09	4.00 ±.09	4.22*		4.88±.2 (10)

+experimental value updated by Meek and Rider
*reference value, rounded off from values in Table 6.

TABLE 12. Cumulative fission yields of rare gas nuclides from thermal neutron-induced fission of Plutonium-239

Nuclide Calculated	Nuclide Measured	Cumulative Fission Yield (%) Reference Nuclides ^{88}Kr	^{88}Rb	^{138}Xe	^{138}Cs	Recommended Mean	Literature Values
^{85m}Kr	^{85m}Kr	0.58 ±.02	0.58 ±.02	0.60 ±.04	0.60 ±.04	0.59	0.598 (2) 0.702±.023 (14) 0.711±.030 (15)
^{87}Kr	^{87}Kr	0.90 ±.01	0.90 ±.02	0.97 ±.05	0.94 ±.05	0.93	0.949 (2)
^{88}Kr	^{88}Kr	1.34*	1.36 ±.02	1.45 ±.07	1.40 ±.06	1.38	1.34 (2)
	^{88}Rb	1.32 ±.02	1.34*	1.44 ±.06	1.39 ±.05		
^{89}Kr	^{89}Kr	1.45 ±.09	1.45 ±.08	1.56 ±.05	1.51 ±.04	1.50	1.44 (2) 1.41±.06 (16)+
	^{89}Rb	1.46 ±.05	1.46 ±.04	1.57 ±.06	1.52 ±.03		
^{137}Xe	^{137}Xe	5.79 ±.34	5.82 ±.29	6.25 ±.24	6.04 ±.12	5.97	6.05 (2) 5.9±.25 (16)+
^{138}Xe	^{138}Xe	4.93 ±.21	4.95 ±.17	5.14*	5.32 ±.14	5.00	5.14 (2) 4.80±1.55 (16)+
	^{138}Cs	4.76 ±.23	4.79 ±.19	4.96 ±.15	5.14*		

+experimental value updated by Meek and Rider

*reference value, rounded off from values in Table 6.

TABLE 13. Cumulative fission yields of rare gas nuclides from fission-spectrum neutron-induced fission of Plutonium-239

Nuclide Calculated	Nuclide Measured	Cumulative Fission Yield (%) Reference Nuclides ^{88}Kr	^{88}Rb	^{138}Xe	^{138}Cs	Recommended Mean	Literature Values
^{85m}Kr	^{85m}Kr	0.61 ±.01	0.61 ±.01	0.64 ±.02	0.59 ±.01	0.61	0.64 (2)
^{87}Kr	^{87}Kr	0.95 ±.02	0.95 ±.01	0.99 ±.04	0.93 ±.01	0.96	1.11 (2)
^{88}Kr	^{88}Kr	1.37*	1.37 ±.03	1.39 ±.05	1.34 ±.03	1.36	1.37 (2)
	^{88}Rb	1.37 ±.03	1.37*	1.34 ±.03	1.33 ±.02		
^{89}Kr	^{89}Kr	1.48 ±.12	1.53 ±.12	1.50 ±.12	1.46 ±.11	1.49	1.65 (2)
	^{89}Rb	1.48 ±.09	1.53 ±.08	1.50 ±.08	1.46 ±.09		
^{137}Xe	^{137}Xe	5.55 ±.18	5.75 ±.09	5.65 ±.12	5.51 ±.14	5.62	5.79 (2) 5.44±1.01 (17)†
^{138}Xe	^{138}Xe	4.48 ±.17	4.65 ±.11	4.56*	4.44 ±.14	4.59	3.86 (2) 4.41±1.82 (17)†
	^{138}Cs	4.66 ±.11	4.69 ±.05	4.68 ±.15	4.56*		

†experimental value updated by Meek and Rider

*reference values, rounded off from values in Table 6.

TABLE 14. Cumulative fission yields of rare gas nuclides from 15 MeV neutron-induced fission of Plutonium-239

Nuclide Calculated	Nuclide Measured	Cumulative Fission Yield (%) Reference Nuclides ^{88}Kr	^{88}Rb	^{138}Xe	^{138}Cs	Recommended Mean	Literature Derived Values
^{85m}Kr	^{85m}Kr	0.82 ±.02	0.82 ±.01	0.75 ±.02	0.77 ±.02	0.79	0.93†
^{87}Kr	^{87}Kr	1.14 ±.02	1.14 ±.02	1.04 ±.03	1.06 ±.03	1.10	1.33†
^{88}Kr	^{88}Kr	1.46*	1.46 ±.03	1.33 ±.04	1.38 ±.04	1.41	1.46†
	^{88}Rb	1.46 ±.03	1.46*	1.35 ±.04	1.37 ±.02		
^{89}Kr	^{89}Kr	1.38 ±.04	1.39 ±.04	1.28 ±.04	1.30 ±.04	1.39	1.32†
	^{89}Rb	1.49 ±.06	1.50 ±.05	1.38 ±.04	1.41 ±.06		
^{137}Xe	^{137}Xe	2.48 ±.05	2.49 ±.05	2.30 ±.11	2.35 ±.06	2.41	4.08†
^{138}Xe	^{138}Xe	1.65 ±.05	1.63 ±.05	1.51*	1.54 ±.03	1.54	2.82†
	^{138}Cs	1.59 ±.04	1.60 ±.03	1.48 ±.03	1.51*		

†chain yield of Nethaway[3] multiplied by calculated fractional cumulative yield of Wolfsberg[4]

*reference values, rounded off from values in Table 6.

nuclide for ^{138}Xe and ^{138}Xe is used for ^{88}Kr. Asterisks are given in the tables for the cases where the cumulative fission yield is equal to the reference value by definition. Since measurement of a daughter activity gives a slightly different result from that of its parent, estimates for ^{88}Kr from ^{88}Kr/^{88}Rb activity ratios and ^{138}Xe from ^{138}Xe/^{138}Cs activity ratios are not quite equal to the chosen reference nuclide yields. For instance, in Table 14 the reference cumulative yield value for ^{138}Xe is 1.51. If the parent-daughter activity ratio was as expected from the half-lives, the measured ^{138}Xe/^{138}Cs activity ratio and its inverse would both also yield a ^{138}Xe cumulative yield of 1.51. Due to experimental uncertainties in determining the parent-daughter activity ratio the values 1.48 and 1.54 were obtained.

The recommended mean value given in the tables is generally the arithmetic mean of the different estimates for the given nuclide. In the case of the reference nuclide ^{88}Kr the recommended mean is the average of the reference ^{88}Kr cumulative yield and the mean of the values obtained with ^{138}Xe as reference nuclide. For instance in Table 14, the recommended mean = [1.46 + (1.33 + 1.38 + 1.35 + 1.37)/4]/2. The ^{138}Xe recommended mean values were derived in the same way.

The uncertainty values shown in Tables 8-14 represent the 1σ variation in the estimates for all the runs of each type. These uncertainty values should be considered as lower limits to the overall uncertainty in the estimates. An uncertainty of at least $\pm$5 percent should be assigned to the recommended mean values due to experimental errors. In many cases the uncertainty in the mean values is larger than this, at least $\pm$ 10 percent, since the

reference nuclide yield values are not well known.

In the event that more accurate values for the cumulative yields of the reference nuclides become available, the experimental results may be updated by multiplication of the recommended mean value by the ratio (new reference nuclide c.f.y. value)/(old reference nuclide c.f.y. value).

A detailed discussion of the values in Tables 13-14 has been given earlier in this report. Discussion of the values in Table 12 was covered in an earlier report[8]. The values reported in Tables 9-11 may have changed somewhat over previously reported values due to additional experimental data and new calibration factors, but the data interpretation presented in the previous report[1] is basically unchanged.

III. ON-LINE MASS SPECTROMETRY

1. Introduction

We have used the technique of on-line mass spectrometry to measure relative independent fission yields for the isotopes of Rb and Cs produced in thermal neutron fission of ^{235}U. Preliminary experiments have shown the possibility of measuring independent fission yields of I and Br by negative-ion mass spectrometry. The on-line technique consists of placing the ^{235}U target material inside a Ta oven which forms the ion source of a mass spectrometer. When the ion source and target assembly is irradiated with neutrons the fission products diffuse out of the target, are ionized on the hot Ta surface and are mass analyzed by a magnetic mass spectrometer.

On-line mass spectrometry was first developed by R. Klapisch and R. Bernas who showed that alkali metal elements diffuse rapidly from hot graphite.[19] These elements are ionized with high efficiency on hot Ta or Re surfaces. When combined with ion pulse counting techniques, the technique has great sensitivity and is rapid enough to measure nuclides with millisecond half-lives.

A. Surface Ionization

For single collisions of neutral atoms with a hot surface, the ratio of the number of atoms leaving the surface as positive ions to the number leaving as neutral atoms is given by the Saha-Langmuir equation:

$$\frac{n^+}{n^o} = \frac{w_+}{w_o} \exp \frac{W - I}{kT}$$

n^+ = number of positive ions

n^o = number of neutral atoms

w_+ = statistical weight for positive ion

w_o = statistical weight for neutral ion

W = work function of metal surface

I = ionization potential of neutral atoms

k = Boltzmann constant

T = absolute temperature

To calculate the expected ionization efficiencies for Rb and Cs we use the value of 4.19 eV for the work function of the Ta surface and the values of 4.18 and 3.89 eV for the ionization potentials of Rb and Cs respectively. The ratio of statistical weights is 1/2 for Rb and Cs. For a temperature of 1500°C, the ionization efficiency $(\frac{n^+}{n^+ + n^o})$ is calculated to be 0.38 and 0.78 for Rb and Cs respectively. These efficiencies are calculated for a single atomic collision with the surface and since multiple collisions are very likely under the target conditions used, the actual ionization efficiencies are even higher. The discrimination against neighboring elements is excellent since they all have higher ionization potentials. For example, the ratios of ionization efficiencies are 6000 and 1000 for Rb/Sr and for Cs/Ba respectively under these conditions. The use of Re with work function of 5.2 eV would give greater efficiencies for Rb and Cs

but would increase the efficiencies for neighboring elements even more. Thus Ta provides the best surface for obtaining high Rb and Cs efficiencies and good discrimination against other elements.

An expression similar to the Saha-Langmuir equation is used to describe the formation of negative ions on a hot surface.

$$\frac{n^-}{n^o} = \frac{w^-}{w^o} \exp \frac{A-W}{kT}$$

n^- = number of negative ions

w^- = statistical weight of the negative ion

A = electron affinity of the neutral atom

The other symbols are defined exactly as given above.

The halogen elements have the highest electron affinities and thus should have good discrimination against other elements when analyzed as negative ions. For Br and I the electron affinities are 3.36ev and 3.06eV respectively and the statistical weight factor is 0.16. At 1500°C on a Ta surface the ionization efficiencies are calculated to be 7×10^{-4} and 1×10^{-4} respectively. Thus the efficiency for Br relative to Rb is lower by a factor of about 500 and the efficiency of I relative to Cs is lower by a factor of about 8000. In addition to the lower ionization efficiencies, the use of negative ions is made even more difficult

due to the problem of thermionic emission of electrons. We have tried to circumvent these two problems by using a surface with a lower work function (i.e., Hf with W = 3.53 eV) to increase the ionization efficiency and by surrounding our oven with a Ta heat shield to prevent thermionic electron emission from interfering with the ion optics. These topics will be covered in more detail below.

B. Targets and Diffusion

The ^{235}U target material was UO_2 powder enriched to 93.15% in ^{235}U. In order to obtain very fast diffusion of Rb and Cs, it is necessary to have the fission products recoil out of the UO_2 matrix and into a graphite matrix. In addition we wished to maximize the amount of ^{235}U in the oven. We therefore intimately mixed equal weights of -325 mesh UO_2 powder with -325 mesh graphite powder. Small amounts of this mixture were placed in a die and were pressed to give thin wafers. These wafers were then cooked at 1200°C for at least 24 hours to give compact samples which could be handled easily without crumbling. Stacks of these wafers were placed in the Ta oven to give the desired amount of target material. The diameter of the wafers was about 10% smaller than the inside diameter of the oven cylinder in order to provide space for diffusion of the fission products. Two different size wafers were used at various times in the course of this work. One set of wafers was 0.34 in. diameter and was used with 3/8 in. diameter ovens. These wafers contained about 50 ±10 mg of UO_2 each. The other size wafers were 0.219 in.

diameter and were used in 1/4 in. diameter ovens. These wafers contained about 25 ±5 mg of UO_2 each. At the temperatures used in these experiments, it is probable that the UO_2 reacted with excess graphite to form UC with some loss of CO and CO_2.

The diffusion of Rb and Cs is much faster in graphite than in UO_2 or UC. It is interesting to estimate what fraction of the fission products can recoil directly out of a particle of UO_2. The maximum particle size for -325 mesh powder is 44μm. If we assume a fission product range of about 7μm and say that all fission products born within 7μm of the surface have a 50% probability of escaping, then we estimate that about 1/3 of the fission products escape from the UO_2 directly due to the kinetic energy in the fission act. For smaller particles, the fraction escaping is considerably greater. It is clear that after the fission products have lost their energy from the fission act, they may be located in a particle of UO_2, in a particle of graphite, or in a void space. In order to reach the hot surface of the Ta oven, the fission products have to diffuse by thermal processes. The diffusion rates are quite different for UO_2 (UC), graphite, or voids. Thus it was necessary to measure the diffusion rates experimentally for each element. This was done by fixing the acceleration voltage and magnetic field for a particular long-lived fission product and recording the ion counting rate as a function of time following a pulse of neutrons. The resulting disappearance curve was fitted to a sum of exponential components by a least-square computer program (CLSQ). Although there is no direct correspondence between the exponential components and diffusion rates

in particular media, the fitting procedure did enable us to obtain effective rate constants and abundances for use in correcting the observed relative yields.

C. Independent Yields

A basic requirement of an independent yield measurement is that the yield of a particular nuclide be measured before beta decay of its precursor has taken place. Because we are dealing with nuclides quite far from stability which have half-lives as short as a fraction of a second, we used pulsed-beam techniques. Fission products were formed during a short pulse of neutron irradiation (about 1 sec) and yields were measured within about 1 sec during and after the pulse.

It should be noted that the mass spectrometric technique did not measure absolute yields. Instead we obtained relative yields of one isotope to another. However, since absolute independent yields are known by radiochemical techniques for some of the longer-lived isotopes, it was possible to normalize our relative yields to the known yields and thus obtain absolute yields for all the isotopes observed here.

The relative yield of one isotope to another was obtained by holding the acceleration voltage constant and sweeping the magnetic field as rapidly as possible over a small range which included the particular masses of interest. Usually only 3 or 4 masses were included in a given mass spectrum sweep so as to restrict the range of counting rates and half-lives. Individual ions were detected by an electron multiplier operated in a pulse-counting mode. Ion-

pulses were recorded in a 400-channel multiscaler whose channel advance was synchronized with the sweeping of the magnetic field. A triangular waveform was used in sweeping the magnetic field and mass spectra were recorded for both sweep-up field and sweep-down field. The sweep-rate was typically about 24 scans per second.

Typical operating conditions for an independent yield experiment are illustrated in Figure 1. The figure shows a neutron pulse lasting 0.5 sec which is repeated 4.0 sec later. The ion current for fission products increases during the neutron pulse and then decreases after the pulse due to diffusion of fission products out of the oven and to radioactive decay of the short-lived isotopes. During the neutron pulse and a short-interval thereafter, the magnetic field is rapidly swept and a "beam-on" mass spectrum is stored in a multiscaler. Just before the next neutron pulse, the "beam-off" mass spectrum is obtained for a time interval equal to the "beam-on" mass spectrum. This cycle of beam-on and beam-off data collection is repeated as long as necessary to accumulate the desired number of events. The number of counts at the top of a particular mass peak in the "beam-on" mass spectrum minus the number of counts at the top of the corresponding peak in the "beam-off" mass spectrum is proportional to the independent yield times a correction factor for diffusion and radioactive decay. The correction factors for each mass number were calculated by taking into account the known radioactive

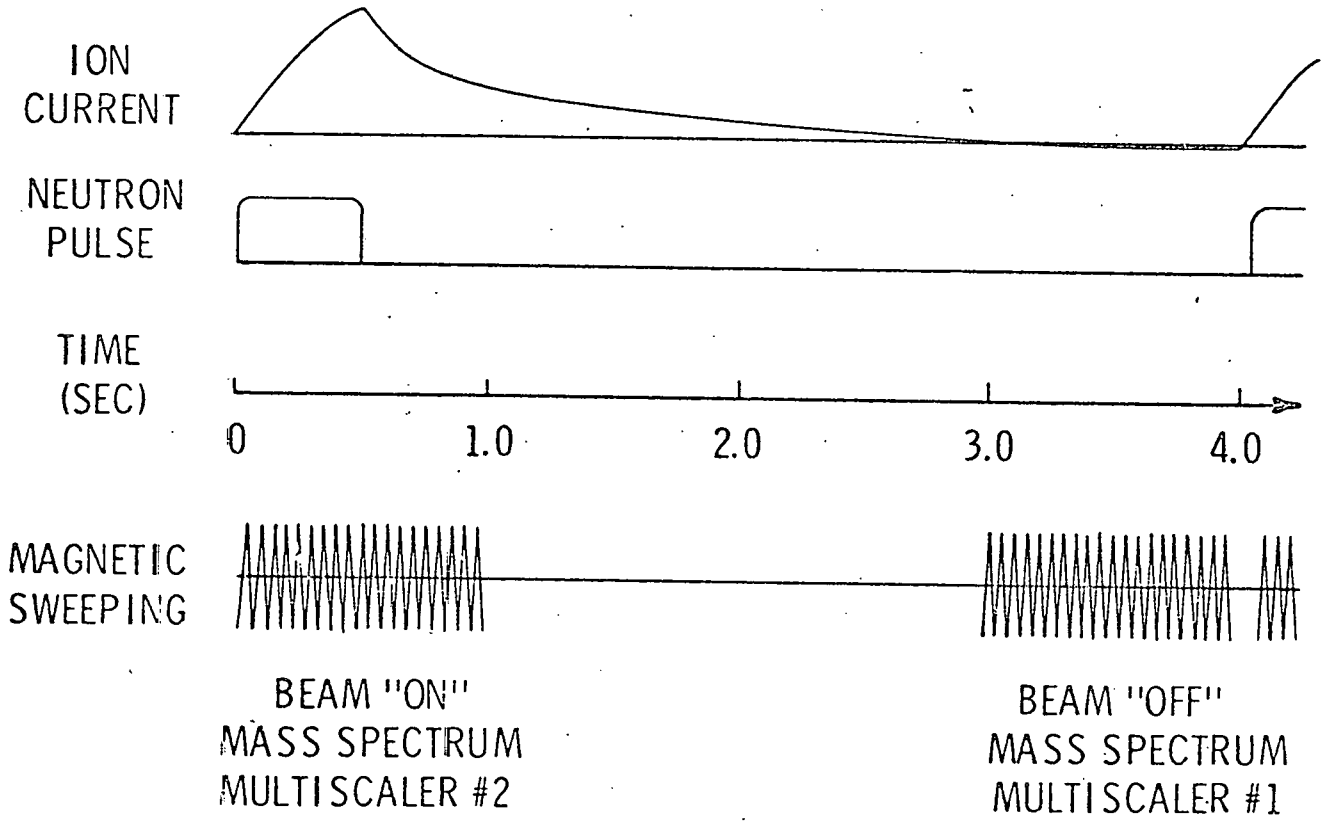

FIGURE 1. Timing characteristics for independent yield measurements. Actual time intervals are adjustable depending on radioactive half-lives and diffusion times to be studied.

half-lives of the nuclide and its precursor, the timing conditions, and the diffusion half-lives and abundances derived from the disappearance curves for each element obtained in separate experiments as described above.

2. Experimental Facilities

Two separate facilities for on-line mass spectrometry were established during the course of this work. The first facility located at Battelle-Northwest Laboratories in Richland, Washington made use of an existing mass spectrometer and a 2-MeV Van de Graaff accelerator for a neutron source. This facility was used for preliminary independent fission yields of Rb and Cs isotopes and for testing of ion-source/target-assemblies for negative ion mass spectrometry. The second on-line facility was specifically designed for installation at a TRIGA reactor located at Washington State University at Pullman, Washington where a 1000 fold increase in neutron flux could be obtained.

A. Van de Graaff Facilities

A schematic drawing of this facility is shown in Figure 2. The Van de Graaff accelerator produced a beam of 2-MeV deuterons which was sent through an 11-foot long beam pipe to a Be target. Fast neutrons produced by the $^{9}Be(d,n)^{10}B$ reaction were slowed to thermal energies in a polyethylene moderator which surrounded the ion-source/target-assembly for the mass spectrometer. The thermal neutron flux at the target position for 100μA of 2.0-MeV deuterons was measured by the gold wire activation method

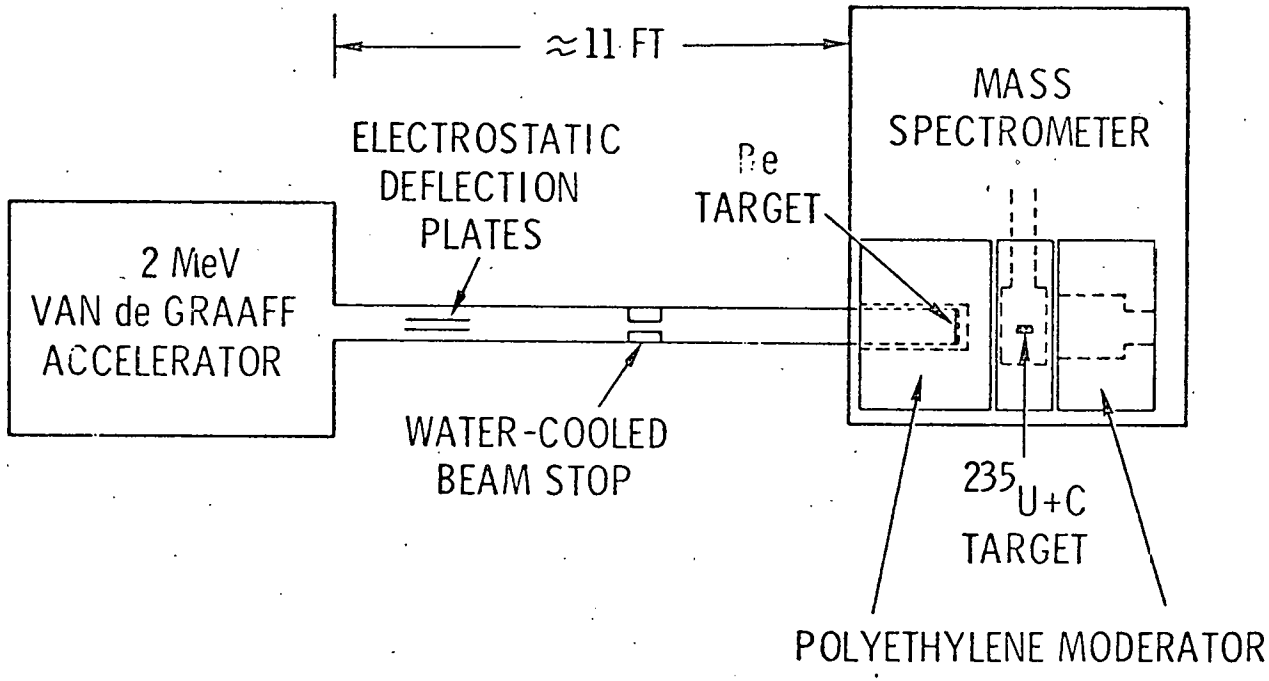

Figure 2. Schematic representation of on-line mass spectrometer system at Battelle-Northwest.

to be about 2×10^7 neutrons/cm^2sec. However, the epithermal flux above the Cd cutoff was about 4×10^7 neutrons/cm^2sec. The large fast neutron flux might have affected the yields of of low-yield products at the wings of the isotopic yield distributions. The neutron flux could be turned on or off by putting a 2-kV potential across the deflection plates in the deuteron beam line. This potential steered the deuteron beam onto a water-cooled copper beam-stop midway along the beam line. The rise time and fall time of the neutron flux was measured by multiscaling the output of a BF_3 ion chamber located just under the polyethylene moderator. These times were of the order of a few millisec. Thus the rise and fall of the neutron flux could be ignored in the correction factors for diffusion and decay.

The mass spectrometer was a simple Nier-type 60 deg. magnetic sector with a 12-inch bending radius. The ion-beam traveled in the vertical plane to an electron multiplier detector located above the beam line. The magnet was a permanent magnet with sweep coils located within the magnet gap to permit scanning the mass spectrum. Scanning rates up to 50 cycles/sec could be used for magnetic field sweeping without seriously distorting the triangular waveform.

B. SOLAR Facility

The Spectrometer for On-Line Analysis of Radionuclides (SOLAR) facility was designed specifically for measurement of independent fission yields with special emphasis on obtaining negative ion-beams of Br and I. Because of the low efficiency

expected for Br and I it was necessary to install the ion-source/target-assembly in as high a neutron flux as possible. In addition we wanted a well thermalized flux to insure that our measured yields were not perturbed by fast neutron fission. The thermal column of the 1 MW TRIGA reactor at Washington State University met these requirements. However, it was necessary to surround the target position with a cadmium shutter in order to achieve pulsed beam operation.

1. Mass Spectrometer

The general layout of the SOLAR facility is shown in Figure 3. The ion-source/target-assembly was located in a hole deep in the graphite thermal column. Ion-beams were brought out through the lead and water shielding by means of an 2.3-meter long evacuated pipe which included two einzel lenses used to focus the beam. The ion beam was bent 90 degrees in the horizontal plane by means of an electrostatic mirror device. Thus the mass spectrometer itself was not located in the radiation field emanating from the thermal column.

The magnet for the SOLAR mass spectrometer consisted of a 45 degree magnetic sector with a 60 degree bend. The ion beam entered and exited the magnetic field at a 7.5 degree angle to the normal. This magnet design was chosen in order to provide some degree of focusing in the Z direction (vertical). A 30% enhancement of the transmission was expected theoretically for this design although no experimental proof of this was attempted.

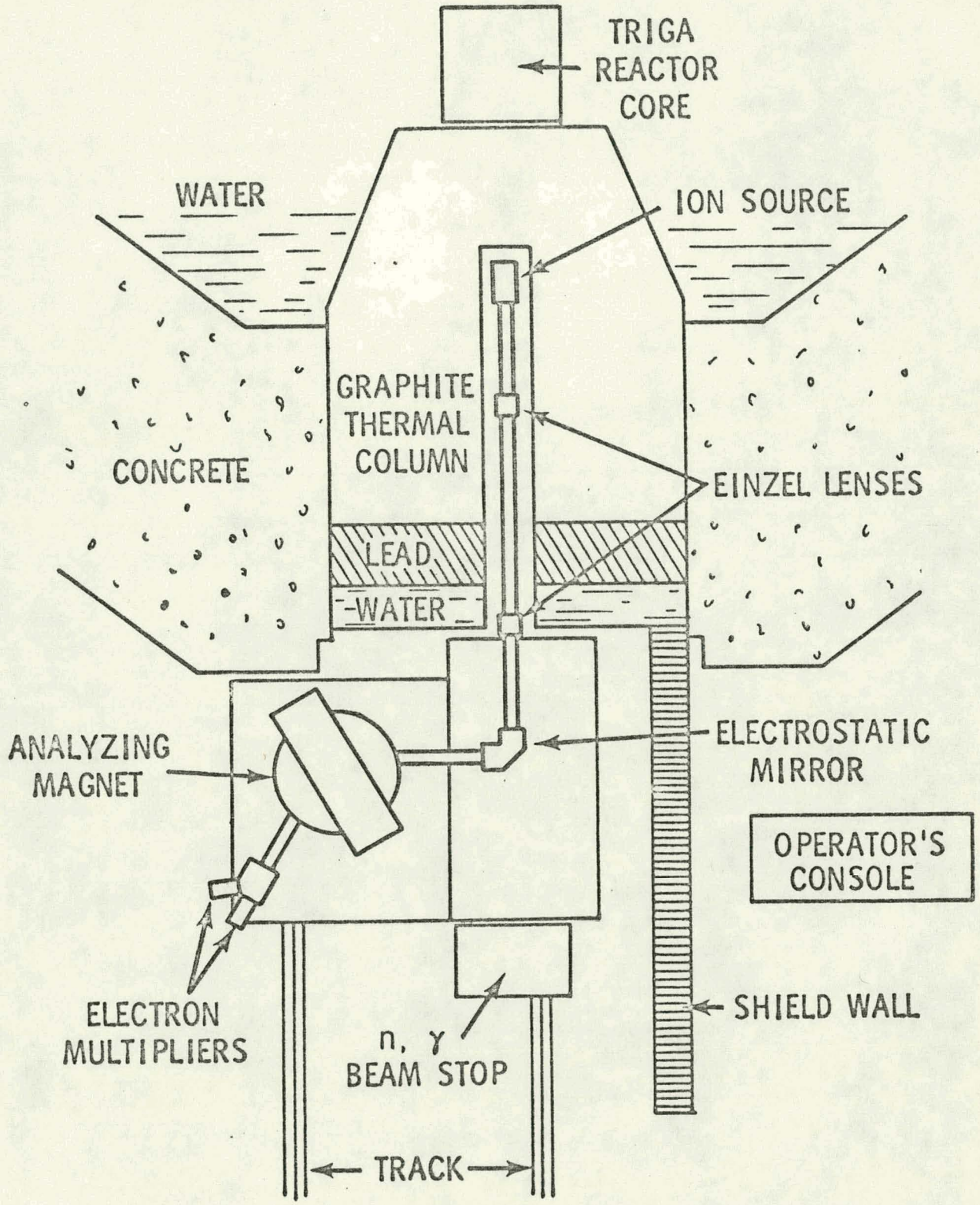

Figure 3. Floor plan of SOLAR facility at Washington State University

The SOLAR magnet was an electromagnet in contrast to the permanant magnet used with the Van de Graaff facility. Thus it was much simpler to reverse the polarity of the magnetic field in switching from positive to negative ions. Magnetic field sweeping was accomplished by separate sweep coils located within the magnet gap. However the distortion of the triangular waveform used in sweeping was more severe with the electromagnet so that the maximum sweep rate used in the SOLAR facility was 24 cycles/sec. instead of 50 cycles/sec which could be used with the Van de Graaff facility.

Two electron multipliers were incorporated into the SOLAR facility for ion detection. One was located on axis with respect to the ion beam leaving the magnet while the other was located 60 degrees off axis. A curved plate electrostatic deflector was used to send the ion-beam to the off-axis detector when desired. Otherwise the ion-beam passed through a slot in the electostatic deflector and entered the on-axis detector. Previous experience with the Van de Graaff facility had shown that the build-up of radioactive atoms on the first dynode of the electron multiplier could lead to a beta particle background which was 10% of the most abundant fission product ion peak. Since this background could interfere with the detection of low yield fission products, we used the off-axis detector for tuning the mass spectrometer on radioactive peaks. The on-axis detector was reserved for actual independent fission yield measurements.

One of the requirements for an "on-line" mass spectrometer is a high transmission efficiency of the ion-beam from the target to the detector. Thus relatively wide slits were used throughout the system to maximize the transmission from a large target. In the SOLAR facility the target material was contained in a 1/4 in. diameter tantalum oven which could be from 3/8 in. to 3/4 in. long. The oven was surrounded by a 1/2 in. diameter heat-shield composed of 10 mil thick tantalum. An 0.020 in. wide "lip" extended from the oven through a slot in the heat shield. This lip protruded 1/32 in. beyond the heat shield and could be from 1/8- to 1/2-in. long depending on the length of the oven cavity. This .020 in. wide lip thus represented the actual source of ions. The ions were accelerated from the oven potential through a Nier-Dietz thick lens to a .024 in. wide slit at ground potential. This slit was the object for the first einzel lens. The first einzel lens brought the ion beam to a focus halfway along the 2.3 meter pipe. This focal point was the object for the second einzel lens which focused the ion beam on the entrance slit of the electrostatic mirror. The entrance and exit slits of the mirror were 0.050 in. which was wide enough to pass most of the ion beam undisturbed. At the exit of the mirror was another .024 in. slit which represented the object for the bending magnet. At the focal point of the magnet was a 0.040 in. slit with the electron multipliers directly behind it. Both the latter two slits could be adjusted in position and width without breaking the vacuum.

The resolution expected for a mass spectrometer with a 12 in. bending radius, 0.024 in. object slit and 0.040 image slit is 175 where resolution is defined as $M/\Delta M$ with ΔM equal to the full width of the mass peak at 1/10 the maxium height. In practice we obtained a resolution of 208 at mass 138. Higher resolution could be obtained by narrowing the object and image slits. However this was not desirable for the independent yield measurements as will be described below in the section on data collection and analysis.

One additional element in the ion-beam flight path was a parallel plate electrostatic deflector located immediately after the object slit at the electrostatic mirror. This provided a correction in the vertical plane in case of a slight deviation from coplanarity in any of the components. This deflector was not ordinarily used since it introduced a defocusing effect and was not necessary when all elements were properly aligned.

Another feature specific for an on-line system was an automatic ion-beam shut off device. This consisted of an electronic switch which could drop one of the beam centering plates in the ion lens-assembly to ground potential when desired. One application of this device was to retain all fission product ions within the ion-source while still maintaining all other components in an operable state. This was useful to prevent unnecessary radioactivity from building up elsewhere in the system. A more direct application was in certain experiments where it was desired to follow the beta decay on the first dynode of the electron multiplier following a short collection of radioactive nuclides.

These experiments could identify the half-life of the nuclide being detected. The procedure was to collect radioactive nuclides of a single mass number on the first dynode, turn off the ion-beam, and then follow the beta decay by storing the counting rate as a function of time in a multiscaler.

2. Radiation Shielding

An on-line facility at a reactor requires extensive radiation shielding from the reactor core while the system is operating and from the induced radioactivity present during and after on-line operation. The WSU reactor operated on a three 8-hour-shifts-a-week basis. This was fortunate for our purposes since this schedule provided ample time for access to the thermal column for installation and check-out of the system. In addition the SOLAR system was designed to fit on a rolling table. Thus the ion-source/target-assembly and flight tube could be pulled out of the thermal column to minimize unnecessary exposure of these components to the high radiation fields. Another feature which helped to reduce exposure of the system was the ability to move the reactor core away from the thermal column when desired.

In spite of these factors, it was still necessary to carefully design the shielding around the SOLAR system to minimize the neutron and gamma radiation fields present in the experimental area during on-line operation. In addition special precautions were required to minimize radiation exposure to personnel during the conversion from on-line to off-line operation and during maintenance procedures for the ion-source/target-assembly.

The flight-tube cadmium-shutter assembly, and ion-source/target-assembly were all designed to fit into a 6-in. diameter hole 57-in. deep within the graphite thermal column. The normal shield for the thermal column consists of a 1/4-in. thick Boral plate followed by a 12-in. thick lead shield, and then a 9-in.-thick water-shield on the outside. Special shielding pieces were fabricated to duplicate these shields but having stepped-diameter coaxial holes for access to the hole in the graphite. Cylindrical graphite, lead and paraffin shields were mounted coaxially on the flight tube to fit snugly into these holes. These latter shields reduced the effective diameter of the hole through the shielding to 3 1/2 in. Additional shielding consisting of a 2-in.-thick lead wall and a 4-in.-thick wall of borated paraffin surrounded the electrostatic mirror. The beam of neutrons and gamma rays emerging from the 3 1/2 in. diameter hole was stopped after the electrostatic mirror by a wall consisting of 12 in. of borated paraffin, 12-in of lead, and finally 4-in. of borated paraffin. The electrostatic mirror was covered by a roof of borated paraffin 4-in. thick. Radiation leakage at the thermal column face was eliminated by an extra shield of lead bricks stacked up from the floor.

A radiation survey was conducted with the shielding in place and the reactor running at full power (1 MW) against the thermal column. The highest radiation field of beta/gamma was 6 mR and the highest neutron radiation field was 3.5 mR. Thus the shielding was quite effective and permitted personnel to walk around the instrument while it was in operation. However, an

additional shield wall constructed from 8 1/4-in thick steel and masonite laminate was placed between the SOLAR facility and the electronic control racks for further reduction of the radiation background at the operations station.

The induced radioactivity of the flight tube, shutter and ion-source/target after a weeks operation of three 8-hour shifts was calculated to be about 10 curies. Procedures have been adopted for handling the facility in spite of these high radiation levels, although such levels have not yet been encountered. The rolling table with the mass spectrometer and part of the shielding can be moved to bring the flight tube, etc., out of the thermal column without exposure to personnel. A 55-gallon barrel with 5-in. thick concrete and 2-in. thick lead walls can then be positioned over the end of the flight tube to provide shielding when the facility is off-line. When the oven and target assembly needs maintenance, the end of the flight tube with the oven flange can be moved into a lucite glove box. The oven flange can thus be removed and manipulated in a controlled environment. The same glove box is used for loading the enriched ^{235}U target wafers into the oven.

3. Neutron Flux Measurements and Cadmium Shutter

Before installation of the complete SOLAR facility, the neutron flux was measured by the gold wire activation technique at the target position and elsewhere in the hole in the thermal column (T.C.). Measurements were made with the reactor core located as close to the thermal column as possible and at a position 6 inches away. Later, another set of measurements was made using

an aluminum cylinder covered with .020 in. thick cadmium to simulate the conditions with the shutter. These flux measurements are summarized in Table 15.

Table 15. Neutron flux measurements at target position in thermal column with reactor at 1 MW.

	Total Flux ($n/cm^2sec.$)	Cadmium Ratio	Thermal Flux ($n/cm^2sec.$)	Fast Flux ($n/cm^2sec.$)
Reactor at T.C.	6.79×10^{10}	19.9	6.45×10^{10}	$.34 \times 10^{10}$
Reactor 6 in. from T.C.	$.46 \times 10^{10}$	14.5	$.43 \times 10^{10}$	$.03 \times 10^{10}$
Reactor at T.C. shutter open	$.80 \times 10^{10}$	3.48	$.57 \times 10^{10}$	$.23 \times 10^{10}$
Reactor at T.C. shutter closed	$.22 \times 10^{10}$	1.02	$.0043 \times 10^{10}$	$.22 \times 10^{10}$

From the data given in Table 15, we see that moving the reactor core 6 in. away from the thermal column reduces the thermal flux by a factor of 15 and the fast flux by a factor of 10.6. We also note that when the cadmium shutter is used, the thermal flux is reduced by a factor of 11.4 from the unperturbed condition.

When the shutter was closed, the thermal neutron flux dropped by a factor of 131 compared to the shutter open condition.

To improve this factor, the actual shutter was then covered with .040 in. thick cadmium and extra cadmium was placed inside the beam pipe to prevent backstreaming of neutrons along the ion-beam path. These improvements led to a final ratio of 800 for the thermal neutron flux with the shutter open to thermal flux with the shutter closed conditions. This latter figure was measured with a small BF_3 counter temporarily mounted at the target position.

The BF_3 counter was also used to give information on the time dependence of the neutron flux when the shutter was opened or closed. The shutter was driven by pneumatic cylinders with a 3-in. stroke. Pure He was used to drive the cylinders. The He flow was controlled by two solenoid valves mounted on the rolling table. After the shutter trigger signal, a time delay of about 40 msec occurred before the shutter began to move. It then took from 80 to 120 msec depending on the He pressure for the shutter to complete its travel. In order to prevent the shutter from hitting the beam pipe too hard, a short burst of He in the opposite direction was given near the end of the stroke to provide a cushioned stop. The time distribution of the thermal neutron flux was obtained by multiscaling the output of the BF_3 counter while the shutter was being actuated. Once the shutter began to move, the neutron flux increased linearly until the maximum opening and maximum flux was achieved. The transit time and hence the rise-time of the neutron flux was comparable to the half-lives of some of the isotopes studied so it was necessary

to take the neutron flux rise-time into account when making corrections to the raw data obtained with the SOLAR facility.

3. Data Analysis

As shown in Figure 1, relative independent yields were obtained in pulsed beam experiments in which "beam-on" and "beam-off" mass spectra were obtained in a cyclic fashion. The difference between the peak intensity in the "beam-on" and "beam-off" spectra had to be corrected for diffusion and radioactive decay. We describe below first how the relative independent yield expressions were derived, next how the diffusion and decay corrections were made and then present the input data consisting of radioactive half-lives, diffusion times and abundances, and calculated fission yield data.

A. Relative Independent Yields

While the neutron beam is on, the ion-current for a particular fission product mass is increasing. The number of ions due to independent production detected during this time interval (t_1) is called N_1. When the neutron beam is turned off, the ion-current decreases due to loss of fission product ions by diffusion and radioactive decay. The number of ions due to independent production detected from the time the neutron beam is shut off to the end of the beam-on mass spectrum (t_2) is called N_2. After an adjustable delay time following the end of the beam-on mass spectrum, a background mass spectrum is obtained

in a separate multiscaler. This beam-off mass spectrum is taken over a time interval equal to $t_1 + t_2$ and the number of ions detected is called N_3. For each time interval there is a corresponding number of ions detected which are produced indirectly by beta decay of the noble gas precursors. These numbers of ions are called N_1^P, N_2^P and N_3^P respectively. The total numbers of counts observed in the beam-on spectrum (A) and in the beam-off spectrum (B) are given by:

$$A = N_1 + N_1^P + N_2 + N_2^P + Bgd + E \qquad \text{(Eq. 1)}$$

$$B = N_3 + N_3^P + Bgd \qquad \text{(Eq. 2)}$$

Bgd is the background due to stable mass peaks and to beta decay of long-lived radioactive isotopes on the first dynode of the electron multiplier. E is the background due to very short-lived radioactivity on the electron multiplier and to gamma-ray induced pulses in the electron multiplier which occur only with the neutron beam on.

We then form the expression

$$A - B - E = (N_1 + N_2 - N_3) + (N_1^P + N_2^P - N_3^P) \qquad \text{(Eq. 3)}$$

where the first term on the right side of the equation contains all the independently produced ions and the second term includes all the ions from precursor decay. Each term N_i can be equated to a quantity $enf\sigma F_i$

where:

e = mass spectrometer efficiency

n = number of target ^{235}U atoms

f = flux of neutrons

σ = cross-section for production of independently formed fission product

F_i = growth, decay, and diffusion factor

Likewise each term N_i^p can be equated to a quantity $enf\sigma_p F_i^p$ where e, n, and f are the same as above, σ_p is the cumulative yield of the precursor, and F_i^p is a growth, decay, and diffusion factor for products of precursor decay. We then obtain the expression:

$$A - B - E = enf\left[\sigma(F_1+F_2-F_3)+\sigma_p(F_1^p+F_2^p-F_3^p)\right] \quad \text{(Eq. 4)}$$

Since enf is a constant, the relative independent yield is given by $(enf)\sigma = \sigma'$ and

$$\sigma' = \frac{A - B - E}{F_1+F_2-F_3+\sigma_p/\sigma\left(F_1^p+F_2^p-F_3^p\right)} \quad \text{(Eq. 5)}$$

We have derived expressions for each of the F factors in terms of the pulsing times, radioactive half-lives, diffusion times and diffusion component abundances. The ratio of precursor cumulative yield to product independent yield (σ_p/σ) is taken from Wahl's calculation

of "normal" fission yields for thermal neutron fission of ^{235}U. (16) All the terms in the denominator can be calculated whereas the terms in the numerator are obtained from the beam-on and beam-off mass spectra. The background term E is given by the difference at the valleys of the beam-on spectrum and beam-off spectrum.

Under ideal conditions, the mass spectrometer gives peaks with flat tops. Since relative peak heights are required (not the area under a peak) a few channels (3-5) at the top of each peak were summed to give the relative number of events at each peak (A,B). The value of E was obtained by summing over the same number of channels at the valley regions and taking the difference between the beam-on and beam-off spectra. This quantity E was due primarily to short-lived beta activity in the case of the SOLAR system since there was very little change in the radiation field at the detector when the shutter was open or closed. The statistical uncertainty in the net counts (A-B-E) was used as a measure of the error associated with a single measurement of a relative yield.

The quantity σ_p/σ obtained from Wahl's calculation is adequate for a first approximation. If necessary the independent yields could be recalculated using the experimental results from the first calculation to estimate the yield ratios.

B. Diffusion/Decay Correction

We give here a brief description of the origin of the diffusion/decay equations to illustrate the nature of this important correction. Because the data reported here were obtained only with the Van de Graaff facility, we can ignore any correction due to the rise and fall time of the neutron flux.

The first step was to derive equations for the number of radioactive atoms of a particular nuclide present in the ion-source as a function of time following the start of a pulse of neutrons. These equations varied according to the time interval of concern. For the Van de Graaff experiments, three time intervals were necessary, one for the period with the neutron flux on, one for the period with the neutron beam off but data still being stored in the "beam-on" mass spectrum, and one for the period of the "beam-off" mass spectrum. The equations for the latter two were essentially identical except for the time range considered.

Each of the equations for the number of atoms present as a function of time included a correction for the buildup of additional atoms from previous neutron pulses. The equations at this stage assumed that a single diffusion component was present.

In addition to the equations for the direct production of radioactive atoms from the independent fission yield, it was necessary to derive additional equations to describe the growth of the radioactive atoms of interest from beta decay of precursor nuclides. Again separate equations were required for each of the time intervals. Thus there were a total of six equations required for the Van de Graaff experiments.

The equations discussed have so far referred only to the description of the number of radioactive atoms present in the source as a function of time with the assumption of a single diffusion rate constant. The next step was to convert these equations

to describe the ion current as a function of time. This was simply done by multiplying the number of atoms present by the diffusion rate constant and the mass spectrometer efficiency factor. The ion-currents corresponding to each diffusion component were then weighted by the relative abundances of that diffusion component. The weighted ion-currents were added to give the total ion-current of that isotope as a function of time.

As described previously, the "beam-on" and "beam-off" mass spectra consisted of a fixed number of rapid scans for each spectrum during each cycle of neutron pulse and data collection. The equations outlined above gave the ion-current of a particular nuclide as a function of time from the start of the neutron pulse to the end of that cycle. Because several masses were covered in each mass scan, the ion-current of a particular mass was not measured continuously, but was sampled at periodic intervals - once during each sweep-up field and once during each sweep-down field. Because of the rapid scanning used, it was assumed that the observed counts at a given mass peak were proportional to the integral of the ion beam-current over the time intervals of mass scanning within each cycle. These integrals over the time factors are the F_i terms appearing in Eqs. 4 and 5.

C. Input Data

In this section we summarize the input data needed for the calculation of the independent fission yields. Tables 16and 17 present the half-lives and fission yield ratios for Rb and Cs

respectively. In Tables 18 and 19 we present the results of diffusion measurements on Rb and Cs. These measurements were performed at the Van de Graaff facility and apply only to the target matrix and temperature specified. Independent yield measurements were performed concurrently with these diffusion measurement so these diffusion parameters are valid for correcting the Van de Graaff yield data.

TABLE 16. Half-life parameters and yield ratios for Rb isotopes in thermal neutron fission of ^{235}U.

Mass	Rb Half-life (sec)	Precursor Half-life (sec)	Yield Ratio[a]
88	1068.	10,080.	78.0
89	900.	186.	14.05
90	210.[b]	32.3	3.72
91	57.4	8.6	1.20
92	4.4	1.84	.424
93	5.9	1.29	.147
94	2.7	1.0[c]	.0507
95	.36	.8	.0162
96	.23	.693[d]	.00524
97	.135	.693[d]	.0016

[a] Yield ratio = Cumulative yield of Kr isotope/Independent yield of Rb isotope. A. C. Wahl's "Normal Yields," 1969.

[b] Composite of isomer half-lives of 156-and 258-sec.

[c] Amiel, et al, report $t_{1/2} = 0.20 \pm 0.01$ sec for Kr^{94} (Ref. 20).

[d] Assumed values.

TABLE 17. Half-life parameters and yield ratios for Cs isotopes in thermal neutron fission of ^{235}U.

Mass	Cs Half-Life (sec)	Precursor Half-life (sec)	Yield ratio[a]
139	558.0	40.0	2.53
140	63.8	13.6	.851
141	24.7	1.72	.304
142	1.7	1.22	.107
143	1.7	.96[b]	.037
144	1.1	.9	.012
145	.56	.9	.004

[a] Yield ratio = Cumulative yield of Xe isotope/Independent yield of Cs isotope. A.C. Wahl's "Normal Yields," 1969.

[b] Amiel, et al, report $t_{1/2} = 0.30 \pm 0.03$ for ^{143}Xe (Ref. 20).

TABLE 18. Diffusion components for Rb at 1580°C (measured at mass 91 only).

Half-time (sec)	Abundance[a]
0.16	0.134
0.57	0.642
4.00	0.176
176.0	0.048

[a] Abundance = $\frac{A_o^i}{\sum A_o^i}$ where A_o^i is the initial count rate of the i-th component.

TABLE 19. Diffusion components for Cs at 1480°C (measured at mass 141 only).

Half-time (sec)	Abundance[a]
0.43	0.11
2.33	0.61
22.2	0.28

[a] Abundance = $\frac{A_o^i}{\sum A_o^i}$ where A_o^i is the initial count rate of the i-th diffusion component.

4. Results

A. Rb and Cs Independent Yields

The independent yield measurements on Rb and Cs reported here are based entirely on experiments done with the Van de Graaff facility. An example of the mass spectra obtained in an independent yield experiment for 400 min. is shown in Figure 4. These spectra were obtained with a beam pulse of 0.4 sec., a scanning time of 0.9 sec., and a delay time of 1.484 sec. The peaks in the beam-off spectrum at masses 93 and 94 are due to residual fission product ^{93}Rb and ^{94}Rb whereas the peak at mass 96 is probably due to a stable isotope. The cycle time in this experiment was only 3.284 sec. which is comparable to the radioactive half-lives of ^{93}Rb and ^{94}Rb. In other experiments the cycle time was set at 6.50 sec. to allow more complete disappearance of the Rb fission products between the beam-on and beam-off spectra.

In Figure 5 we show a similar experiment done with the SOLAR facility for 40 min. In this case the neutron flux was on for 1.0 sec., the scanning time was 0.95 sec. and the delay time was 2.0 sec. It is obvious in comparing the mass 97 peak in the Van de Graaff data and in the SOLAR data that the SOLAR facility provides greater accuracy due to its higher counting rates.

The results for the relative independent yields of Rb isotopes in thermal neutron fission of ^{235}U are shown in Table 20. along with data from other workers for comparison. The column

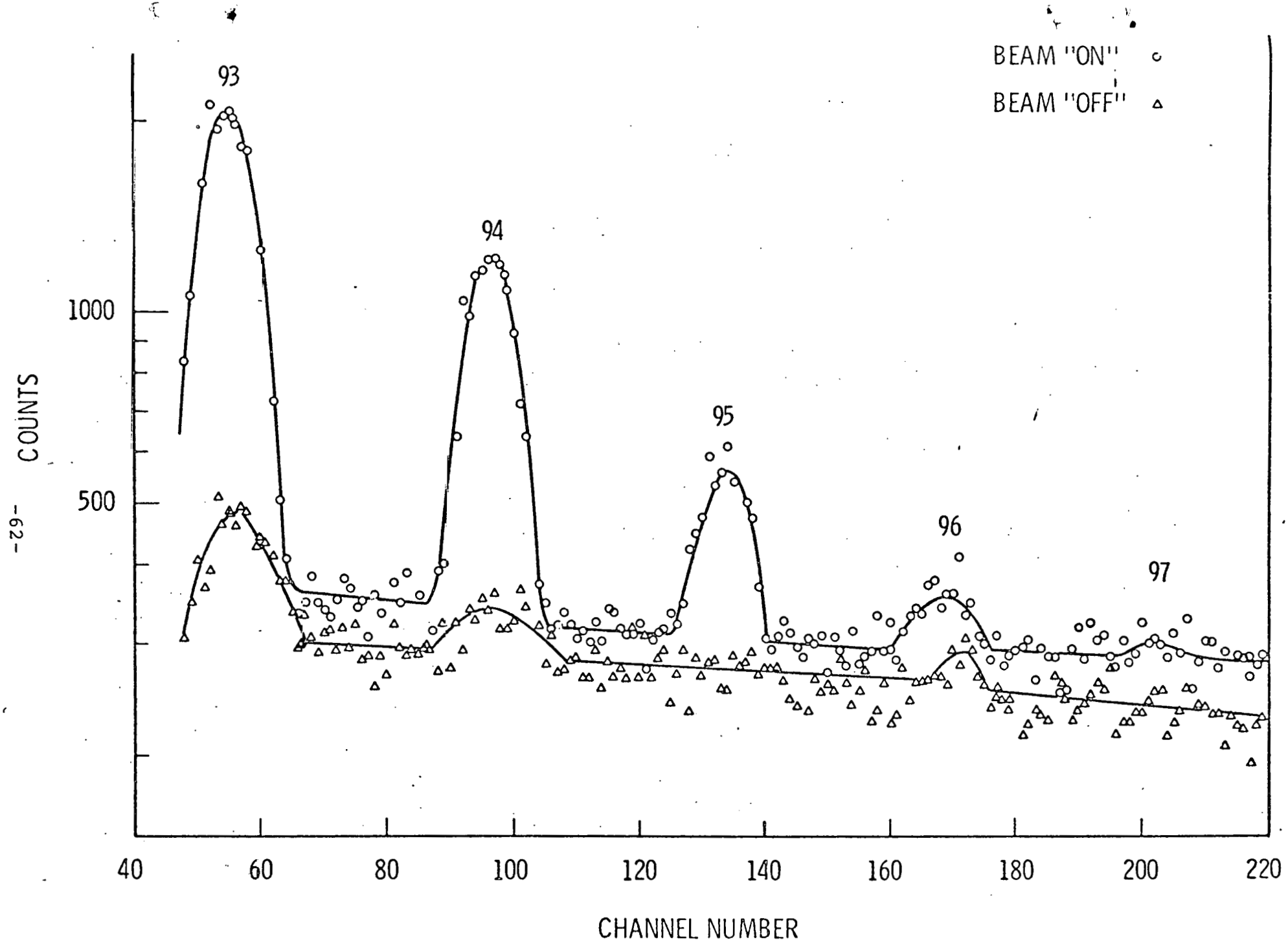

FIGURE 4. Data from indenendent yield measurement of short-lived Rb fission products

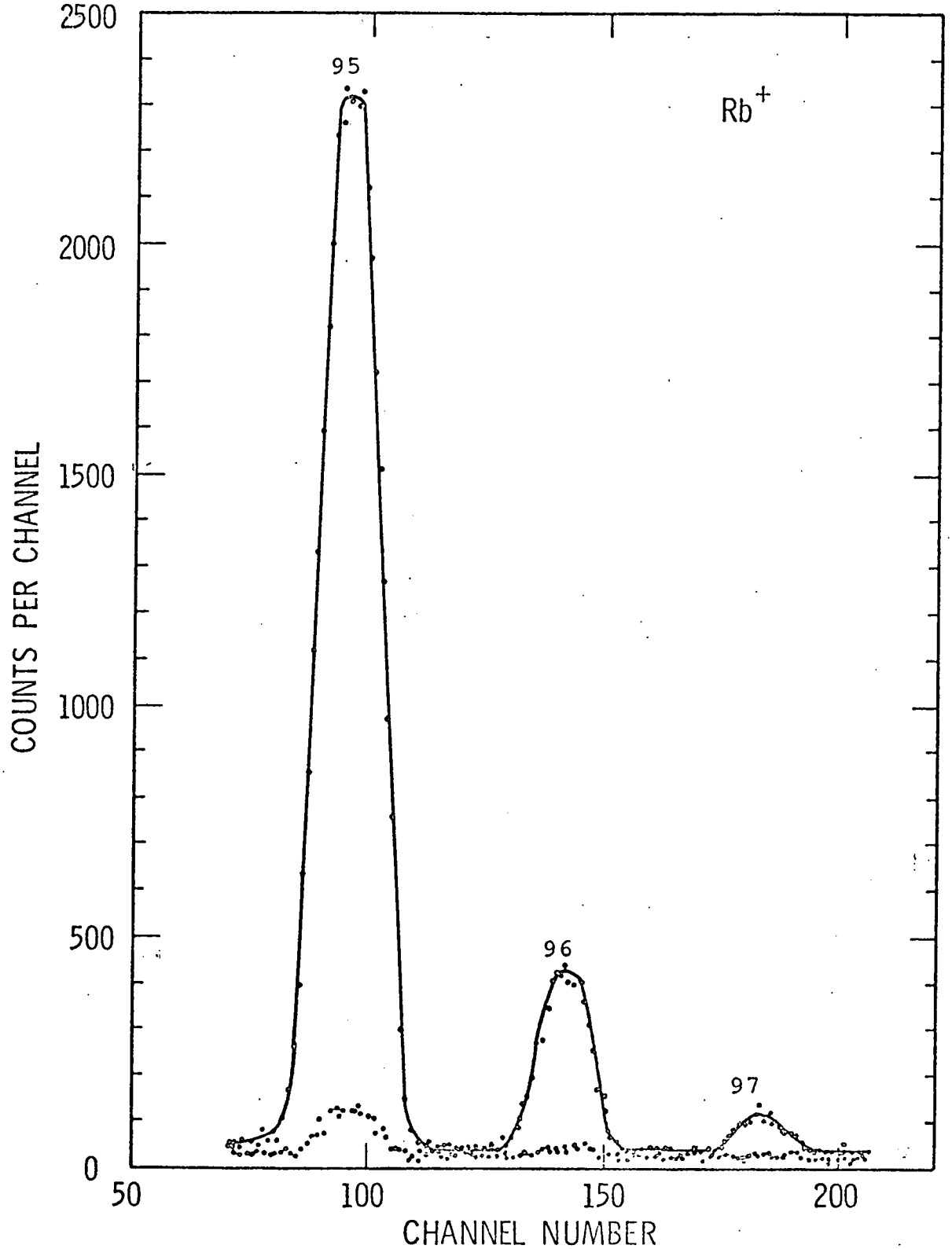

Figure 5. Mass spectra obtained in Rb independent yield experiment at SOLAR facility. Solid curve = beam-on mass spectrum. Dotted curve = beam-off spectrum. Data collection time = about 20 minutes.

labeled Wahl (Calc.) is taken from A. C. Wahl's "Normal Yields" calculated in 1969 based on the best estimates of parameters for a Gaussian charge distribution function.[6] The column labeled Wahl (Exp.) are numbers which Wahl provided to Chaumont[21] and are obtained from radiochemical measurements. The independent yield of the Rb isotopes as reported by Wahl was not measured directly, but was obtained by subtracting the measured Kr cumulative yield and measured Sr independent yield from the total chain yield.

Our experiment is virtually identical to that of J. Chaumont[21] except for the source of neutrons and the U target. There is excellent agreement within the uncertainties for all the experimental data except for our ^{96}Rb and ^{97}Rb yields which tend to be high.

By normalizing our relative yields to the radiochemical yields, we can obtain the independent fission yields in percent. For each isotope from mass 89 to 93, the radiochemically determined yield was divided by the relative yield from the mass spectrometer experiment to give a normalization factor at each mass. The uncertainty in the normalization factor at each mass was calculated statistically and was then applied as a $1/\sigma^2$ weighting factor for the calculation of the weighted average normalization factor. Each relative yield was then multiplied by the weighted average normalization factor to give the independent yields shown in Table 21. The experimental values are all lower than Wahl's calculation of "Normal Yield." This fact has been noted by Wahl,[6] Chaumont[21] and Amiel.[22] It is attributed to a proton paring effect which enhances the yields of even Z elements and reduces the yields of odd Z elements.

The independent yields of Cs isotopes from mass 139 to 145 have been measured in the same manner as for the Rb fission products.

TABLE 20. Relative independent yields of Rb isotopes from thermal neutron fission of ^{239}U.

Mass	Wahl (Calc.)	Wahl (Exp.)	Reeder (Mass Spec.)	Chaumont (Mass Spec.)
89	.086	.060 ± .009	.059 ± .013	.073 ± .024
90	.34	.25 ± .05	.247 ± .015	.25 ± .03
91	.71	.71 ± .10	.732 ± .021	.79 ± .03
92	.99	1.01 ± .20	.937 ± .027	1.10 ± .03
93	1.00	1.00 ± .15	1.000 ± .011	1.00 ± .01
94	.66		.549 ± .009	.51 ± .01
95	.26		.255 ± .008	.22 ± .01
96	.072		.062 ± .009	.044 ± .002
97	.012		.033 ± .011	.012 ± .001

TABLE 21. Independent yields (percent) of Rb isotopes from thermal neutron fission of ^{235}U.

Mass	Wahl (Calc.)	Wahl (Exp.)	Reeder (Mass Spec.)	Chaumont (Mass Spec.)
89	.31	.19 ± .02	.19 ± .04	.22 ± .07
90	1.23	.78 ± .13	.78 ± .07	.75 ± .08
91	2.60	2.25 ± .20	2.31 ± .15	2.37 ± .09
92	3.62	3.20 ± .54	2.95 ± .20	3.29 ± .07
93	3.65	3.17 ± .33	3.15 ± .19	2.97 ± .07
94	2.39		1.73 ± .11	1.52 ± .05
95	.96		.89 ± .06	.64 ± .03
96	.26		.19 ± .03	.131 ± .007
97	.045		.10 ± .04	.035 ± .004

TABLE 22. Relative independent yields of Cs isotopes from thermal neutron fission of ^{235}U.

Mass	Wahl (Calc.)	Wahl (Exp.)	Reeder (Mass Spec.)	Chaumont (Mass Spec.)	Forman, et al. (Mass Spec.)
139	.50	.36 ± .06	.38 ± .03	.49 ± .05	.49 ± .11
140	.90	.75 ± .10	.67 ± .03	.64 ± .04	
141	1.00	1.00 ± .15	1.00 ± .035	1.00 ± .04	1.00 ± .22
142	.84		.95 ± .04	.74 ± .03	.57 ± .18
143	.475		.55 ± .03	.45 ± .02	.38 ± .09
144	.165		.38 ± .04	.09 ± .03	
145	.03		.09 ± .02		.04 ± .02

TABLE 23. Independent yields (percent) of Cs isotopes from thermal neutron fission of ^{235}U.

Mass	Wahl (Calc.)	Wahl (Exp.)	Reeder (Mass Spec.)	Chaumont (Mass Spec.)	Forman, et al. (Mass Spec.)
139	1.82	1.10 ± .14	1.20 ± .12	1.59 ± .15	1.27 ± .19
140	3.29	2.30 ± .21	2.12 ± .17	2.04 ± .12	
141	3.64	3.08 ± .32	3.16 ± .24	3.21 ± .08	2.58 ± .41
142	3.06		3.00 ± .24	2.38 ± .07	1.46 ± .39
143	1.73		1.74 ± .15	1.45 ± .06	.98 ± .17
144	.60		1.20 ± .15	.28 ± .08	
145	.10		.28 ± .07		.10 ± .05

Fission product Cs isotopes below mass 139 are not observed because of the high background from stable isotopes of Ba present as an impurity in the target and oven.

The relative independent yields are presented in Table 22 along with similar data from Chaumont[21] and Forman, et al.[23] Comparison of our results with the other data again shows good agreement for the lighter masses, but our results are higher for the heaviest Cs isotopes (masses 144 and 145).

Conversion of our relative yields to independent yields (percent) was again done by normalization to the radiochemical yields supplied by Wahl to Chaumont.[22] The radiochemical yields as reported by Wahl were obtained as the difference between the chain yield and the sum of the Xe cumulative yield and Ba independent yield in the same manner as for the Rb isotopes. Forman, et al.[23] used a different normalization method so their absolute results are not exactly comparable. The absolute independent yields are given in Table 23.

B. Negative Ions

As mentioned in the introduction the efficiency for negative ion formation of halogens on a hot Ta surface is about 10^3 times lower than for positive ion formation of alkali metals. We thus spent considerable time and effort in searching for ways to improve the negative ion efficiency. In only one experiment at the Van de Graaff were we able to observe Br fission products. This was achieved with a Ta oven surrounded with a Ta heat shield. The counting rate for ^{87}Br was about 20 counts/sec. which was

close to the expected counting rate based on calculated efficiencies. The background was about 10 counts/sec. due to neutron induced background in the electron multiplier detector plus about 25 counts/sec. due to a stable peak in the background mass spectrum. The mass spectrum obtained under conditions of continuous bombardment and continuous sweeping of the mass spectrum is shown in Figure 6. Clear evidence for a difference in beam-off and beam-on spectra between the peak heights of at least three isotopes (87, 88, 89) is shown. These three peaks correspond to the bromine isotopes having the highest expected fission yield under these bombardment conditions. Similar data were obtained for the iodine isotopes but with even lower counting rates, as expected.

Additional data on the Br fission products were obtained 4 days later after cooking the oven and target to reduce background peaks. For this experiment a ^{87}Br counting rate of 120 counts/sec. was achieved with a background continuum of 180 counts/sec. A diffusion curve with poor statistics was obtained at mass 87 and a diffusion time of about 14 sec. was measured. All these Br data were obtained at an oven temperature of about 1500°C.

The large background peaks seen in Figure 6 were attributed to C_n^-, C_nH^- and $C_{n-1}N^-$ ions. These ions apparently are formed by secondary processes involving electron attachment in the gas phase. In later experiments with a small magnet mounted just beyond the oven slit, it was found that stable Br^- and I^- peaks

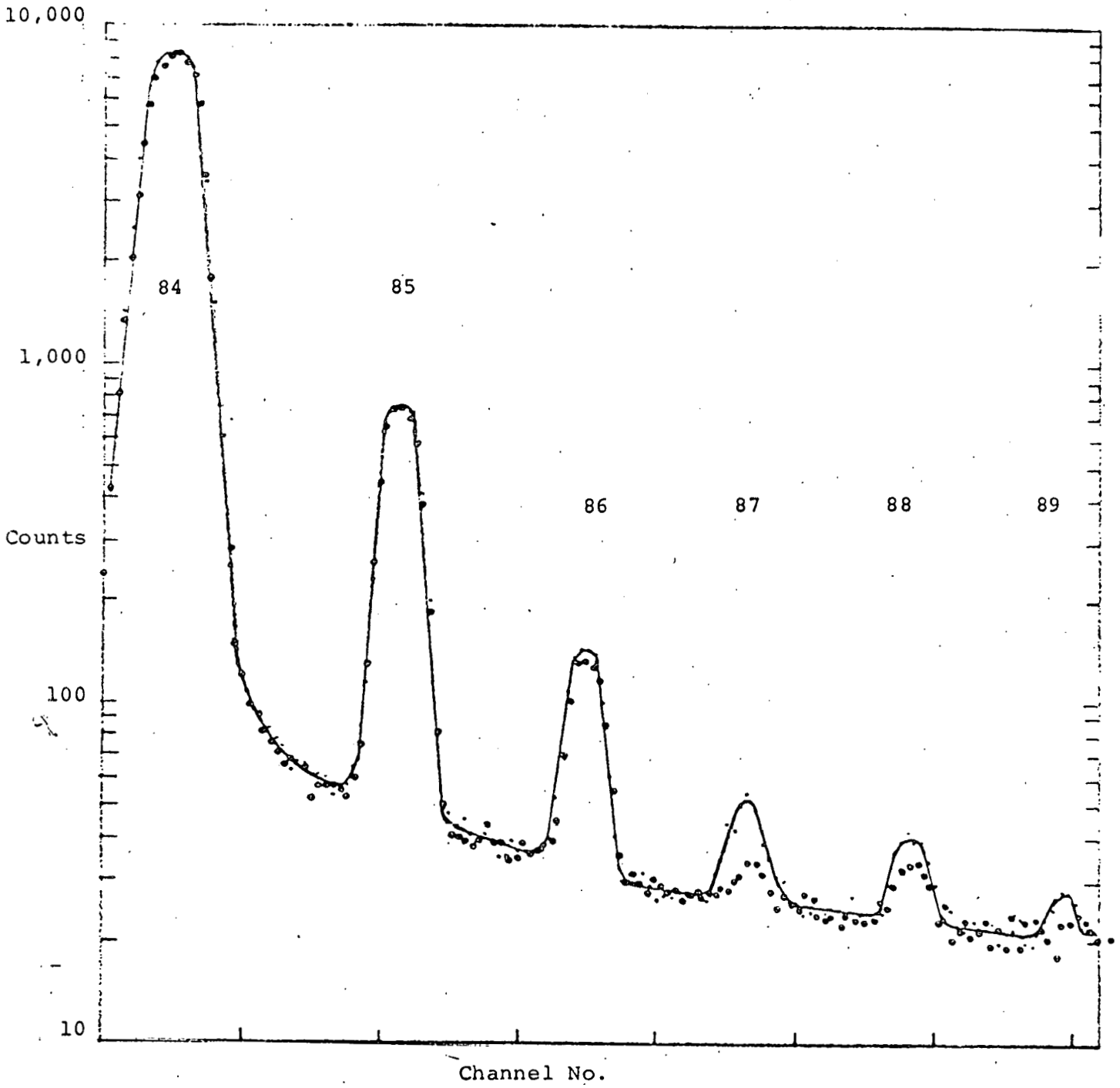

Fig. 6. Mass spectrum of negative ions in Br fission product region. Beam on = ——. Beam off = ····. Beam off spectrum normalized at valleys beside each peak. Run time = 3500 sec on 9-8-72.

were not disturbed by the small magnetic field, whereas the background peaks were greatly altered by the same magnetic field. The magnetic field was installed to prevent thermionic electrons from interfering with the voltages and electric fields of the ion optics. Cutting off the electron current with the magnetic field also cut off the background peaks.

For the oven and heat shield assembly used with the SOLAR system, these background peaks were never seen. This is attributed to the greatly reduced electron current which could only escape from the small region of the lip which protruded through the heat shield.

One possibility for increasing the efficiency for negative ion formation is to use a surface with a low work function. The work function for Ta is 4.19 eV. It would be far better to use a surface with a work function close to or slightly less than the electron affinity of Br and I (3.36 eV and 3.0 eV respectively). A promising candidate for the ionizing surface is Hf. The work function of Hf metal is 3.53 and that of HfC is 2.04. We were not able in the course of this work to obtain fission products Br and I from a Hf surface. However, we were greatly encouraged by the observation of stable isotopes of Se and Te in negative ion mass spectra from a Hf surface. Such peaks were not seen with Ta ovens even at higher temperatures. The electron affinities of Se and Te are about 2.0 eV and thus have a negligible ionization efficiency from a Ta surface. The Se and Te seen in these experiments were present only as impurities in the target and oven materials.

5. Conclusions on On-Line Mass Spectrometric Measurements

The independent fission yields for isotopes of Rb and Cs from thermal neutron induced fission of ^{235}U that are reported here are generally in good agreement with expected values from Wahl's "normal yields" provided the predicted yields are reduced by about 25%. Good agreement with the experimental results of Chaumont is also noted.

The SOLAR facility was designed to provide higher beam intensitities than the Van de Graaff facility in order to measure the Br and I fission products which are less efficiently ionized than the Rb and Cs fission products. The SOLAR facility is now operational and has met its design specifications regarding ion beam transmission, efficiency, and resolution. Measurement of independent fission yields of Br and I with the SOLAR facility appears to be quite feasible.

V. REFERENCES

1. N. E. Ballou, J. H. Kaye, P. L. Reeder, J. J. Stoffels and R. A. Anderl, "Quarterly Technical Progress Report on ARPA Fission Yield Project Work for the Period 1 November 1972 - 31 January 1973," Battelle-Northwest Laboratories Report, BNWL-B-257, March 9, 1973.

2. M. E. Meek and B. F. Rider, "Compilation of Fission Product Yields Vallecitos Nuclear Center - 1972," General Electric Report, NEDO-12154, January 1972.

3. D. R. Nethaway and A. L. Prindle, "Evaluation of Fission Yields for ^{239}Pu Plus 14 MeV Neutrons," Lawrence Livermore Laboratory Chemistry Department Technical Note No. 72-48, September 21, 1972.

4. K. Wolfsberg, private communication, April 1972.

5. N. E. Ballou, J. H. Kaye, P. L. Reeder and J. J. Stoffels, "Quarterly Technical Progress Report on ARPA Fission Yield Project Work for the period 20 April 1972-31 July 1972," Battelle-Northwest Laboratories Report, BNWL-B-207, August 15, 1972.

6. A. C. Wahl, A. E. Norris, R. A. Rouse and J. C. Williams, Proceedings of the Second Symposium on Physics and Chemistry of Fission, IAEA, Vienna, 1969, p 813

7. D. R. Nethaway, private communication, April 1973.

8. N. E. Ballou, J. H. Kaye, P. L. Reeder, J. J. Stoffels and R. A. Anderl, "Quarterly Technical Progress Report on ARPA Fission Yield Project Work for the Period 1 August 1972-31 October 1972," Battelle-Northwest Laboratories Report, BNWL-B-230, November 22, 1972

9. D. C. Hoffman and J. E. Sattizahn, private communication, August 1972.

10. R. Brissot, "Measurement of Fission Yields Using On-Line Isotope Separation," Grenoble Univ. (France), FRNC-TH-92, 1971.

11. K. Wolfsberg, "Nuclear Charge Distribution in Fission: Fractional Yields of Krypton and Xenon Isotopes from Thermal Neutron Fission of U-233 and Pu-239 and from 14 MeV Neutron Fission of U-235 and U-238," Phys. Rev., 137, B929-B935, 1965.

12. L. S. Beller and D. W. Maddison, "Relative ^{238}U Fission Yields by Gamma Ray Analysis," ANS TRANS. 11, No. 2: 607-608, 1968.

13. D. J. Gorman and R. H. Tomlinson, "Cumulative Yields in the 14 MeV Neutron Fission of U-238," Can. J. Chem., 46, 1663-1672, 1968.

14. S. P. Dange, et al., Second IAEA Symposium on Physics and Chemistry of Fission, p. 741, International Atomic Energy Agency, Vienna, 1969.

15. M. V. Raminiah, Private communication to B. F. Rider, June 5, 1971.

16. K. Wolfsberg, Phys. Rev., 139, B304-B-306, 1965.

17. B. M. Moore, "Short-Lived Delayed Gamma-Ray Emission from Fast Fission of Plutonium," LA-4257, October 1969.

18. K. F. Flynn and L. E. Glendenin, "Yields of Fission Products for Several Fissionable Nuclides at Various Incident Neutron Energies," ANL-7749, December 1970.

19. R. Klapisch, J. Chaumont, C. Philippe, I. Amarel, R. Fergeau, M. Salome, and R. Bernas, Nuclear Instr. and Meth. 53, 216 (1967).

20. S. Amiel, H. Feldstein, M. Dron, and E. Yellin, Phys. Rev. 5, 270 (1972).

21. J. Chaumont, Thesis, Faculte des Sciences Orsay (1970).

22. S. Amiel and H. Feldstein, Proceeding of the Third Symposium on Physics and Chemistry of Fission (IAEA, Rochester 1973) paper SM-174/25.

23. L. Forman, S. J. Balestrini, K. Wolfsberg, and T. R. Jeter, International Conference on the Properties of Nuclei Far from the Region of Beta-Stability, CERN 70-30, 589 (1970).

DISTRIBUTION

Advanced Research Project Agency

Col. J. T. Jones (6)

Air Force Technical Application Center

Dr. G. M. Leies (3)

Battelle Northwest

Dr. N. E. Ballou (2)
Dr. J. H. Kaye (2)
Dr. P. L. Reeder (2)
Mr. J. J. Stoffels (2)
Dr. R. A. Anderl (2)
Dr. J. M. Nielsen (1)
Technical Files (4) ✓

Lawrence Livermore Laboratory

Dr. H. G. Hicks (2)

Los Alamos Scientific Laboratory

Dr. J. E. Sattizahn (2)